Role of fruit flesh cell morphology and MdPG1 allelotype in influencing juiciness and texture properties in apple.

Poles L[a‡], Gentile A[bc‡], Giuffrida A[b], Valentini L[d], Endrizzi I[e], Aprea E[e], Gasperi F[e], Distefano G[b], Artioli G[d], La Malfa S[b], Costa F[e,f], Lovatti L[a], Di Guardo M[b]

[a] Innovation Fruit Consortium (CIF), via Mach 1, 38010 San Michele all'Adige, Trento, Italy

[b] Dipartimento di Agricoltura, Alimentazione e Ambiente, University of Catania, via Valdisavoia 5, 95123, Catania, Italy

[c] National Center for Citrus Improvement, College of Horticulture and Landscape, Hunan Agricultural University, Changsha, China

[d] Department of Geosciences, University of Padua, Via Gradenigo 6, 35131 Padua, Italy

[e] Center Agriculture Food Environment University of Trento, Via E. Mach 1, 38010 San Michele all'Adige, Italy

[f] Research and Innovation Centre, Fondazione Edmund Mach, San Michele all' Adige, Trento, Italy

‡: these authors equally contributed to this work

Keywords: X-ray computed micro-tomography; *Malus domestica*; sensory analysis; cellular shape; cellular size; molecular marker

Corresponding author: mario.diguardo@unict.it;

ABSTRACT

Apple fruit quality is strongly influenced by the interplay between juiciness and texture. To better decipher the complexity underneath the control of such quality traits, a multidisciplinary approach combining the mechanic and acoustic profiling of texture, juice analysis, cell morphology, sensory and genetic analysis was carried out. The analyses were conducted after 1.5 months of cold storage on fourteen accessions employed in novel breeding schemes for texture and juiciness. The food matrix structure was exploited focusing on both the cell morphology (employing an optical microscope) and the intercellular space (using an X-ray computed micro-tomography scanner). The mechanical and acoustic properties of texture were profiled with a texture analyser, while the juice was extracted using a mechanical press. In parallel to the analytical assessments, fruit texture, juiciness and flavour were also evaluated by sensory analysis. The results highlighted a positive correlation between cell shape and the intercellular volume. Apple accessions distinguished by round cells were characterized by a reduced intercellular space, while cell with an angular cell shape had a higher intercellular space. While the cell shape was associated with juiciness, the firmness response was more influenced by cell size. The interplay between cellular morphology and juiciness was also investigated together with the allelotype variability of a genetic marker designed for *MdPG1*, a polygalacturonase gene known to control the regulation of fruit texture in apple. The highest juiciness was found in apples with both a high fraction of round cells and the presence of the *MdPG1* allele associated with low softening rates. The elucidation of the role of cellular morphology in the control of fruit texture and juiciness, and their association with the *MdPG1* alleles, provided valuable information for a more detailed and informative analysis of fruit quality, enabling a more precise characterization and selection of superior apple accessions.

1 INTRODUCTION

Fruit quality is affected by appearance, texture, juiciness and nutritional attributes (Abbott, 1999; Cappellin et al., 2015; Corollaro et al., 2014b; Endrizzi et al., 2015). Juiciness and texture have dominant roles in the determination of fruit quality in apple, since these are the two most appreciated characteristics by consumers (Daillant-Spinnler et al., 1996; King et al., 2000; Bourne, 2002).The relative importance of each quality trait component varies greatly among species. These features develop and change during fruit development and ripening processes rendering the fruit desirable and physiologically prone to seed dispersion (Giovannoni, 2004). In apple, the most important changes after colour are fruit softening and increased juiciness. The loss of firmness relies on the depolymerisation of the middle lamellae (a pectin-rich layer adhering cells)-cell wall architectural structure by the action of several cell wall modifying enzymes (CWME) (Brummell and Harpster, 2001). The different types of texture among apple cultivars, depend on the different genetically programmed dismantling events of this polysaccharide structure (King et al., 2000; Waldron et al., 2003). While dry and mealy texture is related to high rate of middle lamellae-cell wall depolymerisation, firm and crispy fruit types are associated with more structured integrity of the cell wall (Longhi et al., 2013b). Fruit texture and juiciness are also related with the types of cell morphology, as documented in tomato (*Solanum lycopersicum*) (Bertin et al., 2001), sweet cherry (*Prunus avium*) (Olmstead et al., 2007) and peach (*Prunus persica*) (Quilot and Genard, 2008). In apple, a direct correlation between cell size, firmness and juiciness was observed in cultivars showing larger cells, which were furthermore characterized by higher levels of juiciness and texture (Allan-Wojtas et al., 2003; Mann et al., 2005; McAtee et al., 2009; Ng et al., 2013). Other work suggests a more complex mechanism of texture and juiciness regulation in which the size and numbers of cells do not have any effect on such quality traits (Charles et al., 2018). To investigate the role of cell morphology in controlling fruit quality aspects, several approaches have been employed, such as light microscopy (Schotsmans et al., 2004; McAtee et al., 2009), scanning electron microscopy (SEM) (Seymour et al., 2002; McAtee et al., 2009; Ng et al., 2013) and X-ray computed micro-tomography scanner (Mendoza et al., 2007; Ting et al., 2013).

Juiciness is the amount of juice released by cell during the breakdown of the cell wall through mechanical compression, and its perception is generally associated with fruit freshness (Corollaro et al., 2014a; Harker et al., 2003). Juiciness can be directly measured as the amount of juice released during either mechanical compression (Corollaro et al., 2014a) or homogenization (Chen and Borgic, 1985; Lill and Mespel, 1988) or indirectly, through the measurement of the juice absorption by a tissue paper, or the weighing of a portion of fruit flesh forced through a Lauer syringe before and after centrifugation (Harker et al., 1997). Fruit texture, is instead considered a multi-trait feature, involving the interplay between mechanical and acoustic components (Costa et al., 2011). Fruit texture has been investigated using texture analysers (Costa et al., 2012). Sensory analysis indicate that fruit texture and juiciness are tightly correlated (Corollaro et al., 2014; Nybom et al., 2003) explaining why texture is often employed as an indirect indicator of juiciness (Allan-Wojtas et al., 2003). Fruit texture and juiciness can be also strongly affected by storage conditions (Corollaro et al., 2013). During storage, in fact, important loss of fruit firmness can occur, severely limiting the storability of particular cultivar and consequently their marketability. For this reason, texture and juiciness are considered as fundamental traits in breeding programs for cultivars with superior fruit quality attributes. The selection process for firmness can now be assisted by molecular markers associated with these traits. For the advanced DNA-informed selection of texture in apple, a gene-based marker related to *MdPG1* has been developed and validated (Longhi et al., 2012, 2013a; Farneti et al., 2017; Di Guardo et al., 2017). This gene is a member of the polygalacturonase family located in chromosome 10 of the apple genome, known to play a pivotal role in the cell wall complex dismantling process (Wakasa et al., 2006).

The objective of this study was to investigate the interactions between cell morphology and texture-juiciness properties, including the *MdPG1* marker allelotype, in fruit of fourteen apple cultivars and selections.

2 MATERIALS AND METHODS

2.1 Plant material

The cultivars and advanced selections used in this study are listed in Table 1 together with their pedigree information. We used cultivars with a history of cultivation and commercialization (e.g. 'Golden Delicious', 'Fuji') and novel accessions chosen for their superior characteristics in terms of fruit quality, production and storability. Five of the accessions included in the list were also used as parental cultivars. Plants were grown in two experimental orchards of the Fruit Innovation Consortium (CIF) located in the province of Trento (north of Italy) and maintained following standard pruning and agronomical practices. Fruit were harvested at the commercial ripening stage, established through the assessment of the starch content on 20 fruit per accession with the Lugol's test (mean value of 7 on the Starch Conversion Chart, CTIFL, Paris, France). For each accession, a minimum of 50 fruits with homogeneous size were collected and stored in air for 1.5 months at 2 °C and 90% relative humidity). After storage, fruit were maintained at room temperature for 24 hours prior the destructive analysis.

Table 1: Cultivars and selections employed in the study. For each accession the parentage is specified; if available, the name of the clone is reported in parentheses next to the cultivar name. The genetic configuration at the $MDPG1_{SSR}10Kd$ locus is reported in the last column both specifying the size of the amplicons (bp) and the favourable (*A*) or unfavourable (*a*) allelic effect on texture.

Accession	Maternal line	Paternal line	SSR-PG
CIV323	Royal Gala	A3-7	313-317 (*AA*)
FEM16	Cripps Pink	Caudle	317-317 (*AA*)
Fuji (Fubrax)	Red Delicious	Ralls Janet	313-313 (*AA*)
Golden Delicious (Clone B)	Grimes Golden	OP	317-324 (*Aa*)
Gradisca	Fuji	Cripps Pink	317-317 (*AA*)
Kizuri	Golden Delicious	NY75413-30	313-317 (*AA*)
Lumaga	Resy	Delbard Jubilee	317-317 (*AA*)
Minneiska	Honeycrisp	Minnewashta	313-317 (*AA*)
MN55	Honeycrisp	MonArk	317-317 (*AA*)
Red Delicious (Jeromine)	NA	NA	313-324 (*Aa*)
Royal Gala (Baigent)	Kidd's Orange Red	Golden Delicious	317-324 (*Aa*)
UEB32642	Golden Delicious	Topaz	317-317 (*AA*)
UEB6581	Fuji	UEB32642	313-317 (*AA*)
Y102	Golden Delicious	SJ109	317-324 (*Aa*)

2.2 Phenotyping of the apple juiciness

For each accession, 10 fruit were used to measure the extractable juice following the protocol described by Corollaro et al. (2014). For each fruit, three disks were isolated from different sides of the fruit (Supplementary Table 1). Extractable juice ('juiciness') was assessed by weighting the liquid expressed from mechanical compression of the disks.

2.3 Texture profiling analysis

Phenotyping of fruit texture was carried-out with a TA-XT texture analyzer (Stable MicroSystem Ltd., Godalming, UK) equipped with an acoustic envelope device (AED) as described by Costa et al. (2011). Mechanical measurements were carried out with a 4 mm flat probe, at a speed of 100 mm min^{-1} and an auto-force trigger at 5 g. The AED connected to the instrument allowed the simultaneous assessment of the acoustic response of the sample during fracturing. Texture properties were measured on three disks/fruit on a minimum of five apples per accession, (Supplementary Table 1). For the combined mechanical-acoustic textural profile, 12 parameters were digitally identified through the use of an *ad hoc* macro (Table 2), as detailed by Costa et al. (2011, 2012).

2.4 Cell isolation and morphological analysis

Three fruits for each accession were selected for cell extraction following the protocol described by McAtee et al. (2009). For each apple, a block with a volume of approximately 1 cm^3 was sampled from the central portion of the fruit cortex, avoiding the cells (normally smaller) located in the proximity of the peel (Allan-Wojtas et al., 2003) (Supplementary Table 1). Sampling was accurately performed by selecting disks at the same depth of the fruit cortex, but the side (sunny and shaded) of the fruit was not taken into account as it does not affect cell size (McAtee et al., 2009). The initial block was further sectioned into smaller cubes of approximately 2 mm^3 using a fine edge scalpel and gently boiled for 25 minutes in a 40 mL solution of 0.05 M Na_2CO_3 in 0.3 M mannitol (McAtee et al., 2009). Mannitol was added to the solution to stabilize the osmotic

pressure, inside and outside the cells, while Na_2CO_3 was added to solubilize the pectin matrix, facilitating the cell separation. This procedure resulted in the dismantling of the ordered cell wall structures while preserving cell integrity and shape. After boiling, single cells formed a homogenate in which cells were suspended in the solution allowing a direct observation or after storage at 4 °C. Cell observation was carried out using a Leica DM 2500 optical microscope (Heidelbergh, Germany) equipped with a Leica DFC 320 digital camera and a 10x magnifying glass under bright field. Cell images were elaborated and analysed using the Leica application suite software (v. 2.5.0). Each cell contour was manually highlighted enabling the software to automatically compute the corresponding cell area (CA), perimeter, height and width. Cellular shape (CS) was instead indirectly determined through the analysis of the ratio between height and width, following the assumption that more similar these two parameters are, more round the shape of the cell will be, as already proposed by Smedt et al. (1998). Both raw and processed photos are available upon request.

2.5 DNA extraction and analysis of *MdPG1*

For each accession included in this survey, total genomic DNA was isolated from young leaf tissue using the Qiagen DNeasy Plant mini kit (Qiagen) following the manufacturer's protocol. DNA quality was assessed using a Nanodrop ND-8000® spectrophotometer (Thermo Scientific, USA). For each sample, the genetic configuration at the $MdPG1_{SSR}$10kd (the molecular marker designed to target the *MdPG1* gene) locus was assessed using the primer sequences and PCR conditions described by Longhi et al. (2013a). $MdPG1_{SSR}$10kd was amplified using the following pair of primers: forward:_5'-50-TTTCTTCCTTGGGTTTTTGG-3' and reverse_5'-ACTCGTGCGCCAGATAGC-3' The PCR amplification thermal conditions were: 94 °C for 2 min, 32 cycles of 94 °C for 30 s, 58 °C for 30 s and 72 °C for 45 s, followed by a final extension of 72 °C for 5 min. PCR products were separated using an ABI Prism 3730 capillary sequencer (Applied Biosystem by Life Technologies) while the size of the amplicons was assessed using the GeneMapper® software (Applied Biosystem by Life Technologies).

2.6 X-ray computed micro-tomography

3D imaging was carried out on a restricted dataset encompassing the two MDPG1$_{SSR}$10Kd genotypes in analysis and, within each genetic class. 'Fuji', 'Kizuri', 'Gala', 'Golden Delicious', 'Gradisca', 'Lumaga' and 'Minneiska' were selected on the basis of their divergent juiciness and texture responses. The measurements were performed using a Skyscan 1172 micro-CT scanner. Cylindrical cores of approximately 6 mm diameter and 20 mm height were extracted and mounted on a plastic sample holder (Supplementary Table 1). The samples were irradiated using a cone-shaped X-ray beam (W source) with 44 kV voltage and 222 µA current. Each projection was acquired with an exposure time of 265 ms and an angular step of 0.3°. Tomographic reconstruction was performed using the FDK algorithm (Feldkamp et al., 1984). After this latter step, the dataset associated with each cultivar consisted of a sequence of 1,200 cross sections having a pixel size of 5 µm. These images were cropped at a final diameter of 4 mm in order to remove any possible artefact deriving from sample extraction. Binary images were obtained using an iterative thresholding method (Ridler and Calvard, 1978) and analysed using the Fiji software (Schindelin et al., 2012) to measure the volume of the individual intercellular spaces (IS).

2.7 Sensory analysis

The **s**ensory profiles of apples were assessed using the descriptive analysis method with a consensus lexicon of 34 sensory descriptors developed by Corollaro et al. (2013). We considered nine descriptors related to texture, juiciness aroma and flavour. The latter two were included in the analysis in light of their relationship with texture and juiciness characteristics (Supplementary Table 2). The intensity of each descriptor was expressed as a score on a 100 mm linear scale, ranging from 0 (absence) to 100 (extremely intense), and with 50 as middle point. The analyses were carried out by a trained panel composed of 15 panellists (8 males and 7 females) who had between 2 and 7 years of experience in descriptive analysis of apple fruit quality aspects. Fruit were analysed in five panel sessions according to the different harvest dates. Panellists evaluated 3 apple samples per session in duplicate according to a balanced order of presentation over the panel. Each

panellist received eight apple disks per apple sample: flesh cylinders (1.8 cm diameter; ±2.5 g) cut from 8 different fruit (Supplementary Table 1), treated with an antioxidant solution (0.2 % citric acid, 0.2 % ascorbic acid, 0.5 % calcium chloride), and presented in a clear plastic cup encoded with a random three-digit code. The panel evaluated the samples under red light (to avoid bias due to the external appearance of the sample) in a sensory laboratory equipped with 22 individual booths. Refer to Corollaro et al. (2013) for further details regarding the selection of the panel and its performance monitoring, general lexicon development, and evaluation procedures.

2.8 Statistical analysis

The outputs of the different analyses were processed, integrated and visualised using the R software (R Core Team, 2016). Tables of correlation were visualized using 'psych' package (Revelle, 2017), principal component analysis (PCA) were calculated using the 'prcomp' function of the 'stat' package; outputs were displayed using the 'factoextra' package (Kassambara and Mundt, 2016). Heatmaps were produced using the packages 'ggplot2' and 'Deducer' (Fellows, 2012; Wickham, 2016) and the 'cor' function of the 'stat' package.

3 RESULTS

3.1 Phenotypic analysis of juiciness and fruit texture in apple

'Juiciness' was assessed on 10 fruit (3 disks/fruit) per accession through mechanical extraction. The 'juiciness' measured across the 14 accessions showed a normal distribution (Shapiro-Wilk test: W = 0.99, p value = 0.52), with a mean and median value of 3.12 and 3.13 g, respectively. Significant differences were observed among accessions (ANOVA test: F value = 12.5, p value < 2.2^{-16}; Figure 1A), with 'Lumaga' and 'MN55' showing the lowest (2.75 g) and highest (3.42 g) juice mean value, respectively (Figure 1A, Table 2).

The fruit texture of the 14 accessions was phenotypically analysed through the identification of 12 parameters related to both the mechanical and acoustic component of texture (Supplementary Figure 1, Table 2). All traits showed a quantitative distribution and the pairwise correlations between parameters ranged from 0 (absence of correlation, as observed for 'Yield force' and 'N. Force Peak') to 1 (perfect correlation, for 'Mean force' and 'Area') (Supplementary Figure 1). For group of parameters with a correlation higher than 0.97, only one was considered for further analyses, thereby reducing data redundancy. Therefore, 'Area' and 'Mean force' were not further considered since both had correlations of 0.97 with 'Max force' (included in the analysis) (Supplementary figure 1).

The 10 remaining parameters were used for principal component analysis (PCA) to get insights on the texture differences between samples (Supplementary Figure 2A-B). The combination of the first two PCA dimensions (Dim1 and Dim2) explained a total phenotypic variability of 93.1 % (Dim1 = 73.1 %, Supplementary Figure 2C) providing an accurate overview of the different texture performances among accessions. Dim1 was linked to the overall textural performance and allowed the identification of two main groups, with samples showing low or high textural properties characterized by negative or positive Dim1 values, respectively (Supplementary Figure 2A); to this extent 'Gala' and 'FEM16' showed the highest (4.33) and lowest (-4.09) PC1 values respectively (Supplementary Table 3). These insights were complemented by Dim2 (20 % of the total variability) that allowed a clear distinction of accessions according to the acoustic or mechanical components of texture (respectively red and blue arrows in Supplementary Figure 2B). Cultivars showing

positive Dim2 values (‘Lumaga’ PC2 = 2.94) were characterized by firmer texture while a negative Dim2 (‘Kizuri’ PC2 = -1.79) identified accessions with a high acoustic response (Supplementary Figure 2A-B; Supplementary table 3). The two traits showing the highest divergence in terms of Dim2 loading scores were the ‘Final force’, representative of the mechanical component, and the ‘N. Force Peak’ (supplementary Figure 2B). Even though the latter was formally considered a mechanical parameter, previous reports have highlighted its strict correlation with acoustical parameters (Costa et al., 2011). The comparison of the phenotypic distribution of the two divergent traits (Supplementary Figure 2D-E) showed substantial differences in the mechanical and acoustic behaviour of the different accessions with ‘Lumaga’, for instance, showing the highest mean value for ‘Final force’ and the second lowest value for the ‘N. Force Peak’ (Table 2).

Table 2: Instrumental measurements of juiciness, texture and cellular morphology for the fourteen accessions in analysis. The phenotyping of texture involved the analysis of twelve traits either related to the mechanical or acoustic component of texture. Cell morphology was analysed focusing both on cell area (CA) and cell shape (CS). Measure units are specified in brackets (g = grams, N = Newton, dB = decibel, m = meters).

Accession	'Juiciness' [g]	Yield Force [N]	Max Force [N]	Final Force [N]	Mean Force [N]	Area [N *Strain]	Force Lin. Dist.	Young's Module [N*Strain]	N. Force Peak	Max Acoustic Pres. [dB]	Mean Acoust. Pres. [dB]	Acoust. Lin. Dist.	Acoust. Peak	CA [μm^2]	CS
Lumaga	2.75	12.4	16.6	14.0	13.6	1,148	106.2	1.6	26.4	58.1	32,858	5,203	626.7	43,858	1.309
FEM16	2.81	11.1	15.7	12.4	12.9	1,106	122.4	1.9	35.6	64.4	32,897	7,858	830.0	41,562	1.302
Gala	2.99	7.6	9.2	6.9	7.6	656	99.9	1.2	23.3	54.2	32,833	2,716	281.1	36,051	1.269
UEB32642	3.00	10.1	11.4	8.5	9.7	822	104.4	1.2	26.8	59.4	32,844	5,334	528.0	48,528	1.334
Golden Delicious	3.02	6.4	7.9	5.9	6.5	566	100.5	1.3	27.9	57.5	32,840	4,420	477.1	34,642	1.262
Red Delicious	3.11	5.9	8.0	6.3	6.6	568	102.0	1.2	31.9	57.4	32,860	5,057	612.4	34,719	1.233
Gradisca	3.12	9.1	12.6	8.7	10.5	900	114.4	1.8	34.7	63.2	32,885	7,475	823.8	34,318	1.272
CIV323	3.15	10.5	13.3	11.1	11.2	954	107.0	1.4	27.9	58.1	32,847	4,170	480.6	33,137	1.310
Y102	3.17	10.8	13.3	8.9	11.0	945	111.5	1.7	31.7	61.2	32,864	5,794	658.3	35,356	1.186
UEB6581	3.19	12.7	15.5	12.8	13.2	1,124	111.9	1.5	31.5	61.9	32,869	6,109	702.3	43,171	1.271
Minneiska	3.28	5.8	7.2	5.4	6.0	517	99.5	1.0	28.3	56.0	32,848	3,172	425.0	38,465	1.235
Fuji	3.31	8.7	11.1	8.4	9.4	807	107.5	1.5	31.6	61.9	32,880	6,630	764.9	41,109	1.272
Kizuri	3.39	10.4	12.6	8.0	10.3	878	123.2	1.5	35.4	66.6	32,899	8,988	824.8	38,731	1.184
MN55	3.42	10.6	13.0	10.7	11.2	965	110.8	1.7	32.9	64.5	32,886	7,333	792.1	44,457	1.206

3.2 Histological analysis of the flesh tissue in different apple varieties

The analysis of the cell morphology (CA, perimeter, width and height) was conducted on all accessions. Since CA and perimeter showed a high positive correlation (cor = 0.9, p value = $< 2^{-16}$), only CA was further considered for analysis. A lower, though significant, correlation was instead observed between CA and Width (cor = 0.68, p value = $< 2^{-16}$) as well as between CA and Height (cor = 0.66, p value = $< 2^{-16}$), while no correlation was instead observed for Width and Height (cor = 0.09, p value = 9.272^{-10}) (Supplementary Figure 3).

The number of cells analysed varied from 199 for 'UEB6581' to 343 for 'Gradisca' (mean and median equal to 271 and 272 cells per accessions respectively) according to the different efficiency in the cell extraction procedure (Supplementary Figure 4). To assess if the number of cells analysed was sufficient for robust estimates, 1000 subsets (represented by 10 different subset sizes with 100 repetitions each) for each accession were randomly sampled from the total number of cells and the relative mean CA calculated. The subset sizes were established by dividing the range between 10 cells (arbitrarily set as the minimum sample size to calculate a mean value) and the total number of cells in ten uniform intervals. For each subset size, 100 random samplings were performed, and the respective mean CA value calculated. As expected, the CA mean variability within the 100 repetitions decreased with the increase in size of the subset. For all accessions, 100 randomly chosen cells provided already a robust estimate of the overall CA (Supplementary Figure 4). The same process was also performed for perimeter, width, height and CS giving similar results (data not shown).

Overall, the CA distribution showed a quantitative, slightly skewed, distribution, with mean and median values equal to 39,653 and 38,390 μm^2 respectively (Table 2). Significant differences between accessions were observed (ANOVA test: F value = 51.45, p value $< 2^{-16}$). Among the fourteen accessions, 'CIV323' and 'UEB32642' showed the lowest and highest median CA values (33,137 and 48,528 μm^2), respectively (Figure 2A, Table 2). The cultivars standard deviation was normally distributed (Shapiro-Wilk test: W = 0.97, p value = 0.88) with extreme values ranging from 9,912 ('Y102') to 15,505 ('Minneiska') (Figure 2A). CS showed

instead a skewed distribution with mean and median value equal to 1.35 and 1.25, respectively (Table 2). Differences in CS among cultivars were observed (ANOVA test: F value = 8.75, p value < 2^{-16}), with 'Kizuri' and 'UEB32642' showing the lowest and highest median value respectively (1.184 and 1.334 respectively, Figure 2B). As for the CA, the cultivar standard deviation was normally distributed (Shapiro-Wilk test: W = 0.92, p value = 0.22). The standard deviation for CS was larger in cultivar showing higher CS (thus a higher fraction of angular cells), with 'Kizuri' and 'UEB32642' showing not only the most extreme CS values but also the lowest and highest standard deviations (Figure 2B).

3.3 Combined analysis of 'juiciness', textural properties and cellular characteristics

The texture parameters, together with juiciness and cell morphology related traits, were distributed over a 2D-PCA plot (Figure 3, Supplementary Table 3). The first two dimensions explained a cumulative phenotypic variability of 80.9 %. Dim1 (57.3 % of the total variability) was predominantly influenced by individuals with poor texture, such as 'Gala' (PC1 = 4.48) and 'Minneiska' (PC1 = 3.82) plotted in the Dim1 positive area, as well as accessions showing desirable textural features like 'FEM16' and 'Kizuri', distinguished instead by negative Dim1 values (PC1 = -3.97 and -3.53 respectively) (Figure 3A, Supplementary Table 3). PC1 scores were associated with all texture parameters, with 'Max Acoustic Pressure' (cor = -0.95, p values = 0.51^{-7}) showing the highest association, while neither CS, CA nor 'juiciness' showing significant associations with PC1. Similarly to what observed on supplementary Figure 2B, the mechanical and acoustic properties of texture can be efficiently discriminated through the examination of the Dim2, with individuals showing high firmness ('Lumaga', PC2 = 3.65) or favourable crispness ('Kizuri', PC2 = -2.55) and characterized by the highest positive and negative Dim2 values, respectively (Figure 3A). In addition, the orientation of the accessions along the y-axis was greatly influenced by 'juiciness' and CS (Figure 3A). Both traits, although in opposite directions, showed a projection over the y-axis. However, while the loading representing 'juiciness' directed towards the lower-left quadrant, the CS loading was oriented towards the specular upper-right quadrant (Figure 3A). The visual inspection of the 2D-PCA plot underlined that juiciness and round shape type of cells were distinguished by negative values of Dim2, while elongated type of cells and more dried fruit were

297 characterized by positive values of Dim2. PC2 scores showed the highest correlation with 'juiciness' (corr = -
298 0.76, p value = 0.001) and 'CS' (corr = 0.81, p value = 0.0004). The opposite projection of 'juiciness' and CS
299 loadings underlined an inverse correlation between these two traits, suggesting a direct role of the cellular
300 shape in modulating the juiciness response. This result was further confirmed by the heatmap depicted in
301 Figure 3B, with CS and 'juiciness' showing an inverse correlation (cor = -0.68, p value = 0.007) (Figure 3B). In
302 contrast to what was observed for CS, CA showed a direct correlation with firmness parameters (and not
303 with 'Juiciness') as indicated by its loading orientation with regards to 'Final force', 'Max force' and 'Yield
304 force' (Figure 3A) and correlation values ranging from 0.41 ('Max force') to 0.49 ('Yield force') (Figure 3B).

305

306 **3.4 Interplay between 'juiciness', CS and the MDPG1 SSR10Kd marker**

307 Previous work have highlighted the central role of the cell wall modifying enzyme *MdPG1* in modulating
308 textural characteristics (Longhi et al., 2012, 2013a; Di Guardo et al., 2017) but associations between juiciness
309 and *MdPG1* has not been investigated. To test this hypothesis, the apple accessions were genotyped with
310 the *MDPG1*$_{SSR}$10Kd, an SSR marker closely linked to *MdPG1* (Longhi et al., 2013a). The MDPG1$_{SSR}$10Kd
311 genotypes where distinguished by three alleles, consistent with the findings previously reported by Longhi
312 et al. (2013a). The two alleles 313 and 317 were previously associated to a favourable textural characteristics
313 (A), while the 324 bp-allele was instead associated with a poor textural performance (a) (Longhi et al., 2013a,
314 2013b; Baumgartner et al., 2016). The presence of two *A*and one *a* alleles allowed the distinction of the apple
315 accessions among three genotypic classes (*AA*, *Aa* and *aa*). The apple accessions considered in this work were
316 represented by 10 AA and 4 Aa genotypes (Table 1). MDPG1$_{SSR}$10Kd was associated with all 10 textural
317 parameters (Welch Two Sample t-test, p values ranging from 4.52^{-5} to < 2.2^{-16}, Supplementary figure 5) while
318 no significant association was found for MDPG1$_{SSR}$10Kd allelism and 'juiciness' (Welch Two Sample t-test, p
319 value = 0.11), implying that MDPG1$_{SSR}$10Kd alone could not be associated with juiciness (Supplementary
320 Figure 6).

The role of MdPG1$_{SSR}$10kd in controlling juiciness was also analysed together with CS, the only parameter showing a significant correlation with 'juiciness' (Figure 4). 'MN55' and 'Kizuri' had the highest 'juiciness' and the lowest CS values (thus the highest fraction of round cells), while 'Lumaga' and 'FEM16' were characterized by a specular phenotype, with lower 'juiciness' and higher CS values (Figure 4). The fitted line (grey line in Figure 4) represented the optimal regression line linking CS with 'juiciness'. All apples plotted below or above the fitted line were characterized by lower or higher 'juiciness' responses respectively, with regards to their cellular morphology. It is interesting to notice that none of the accessions plotted above the fitted line (higher 'juiciness' compared to CS) showed the *Aa* MdPG1$_{SSR}$10kd allelic state. The relationship between the marker allelism and juiciness was further supported by the comparison between the 'juiciness' of accessions showing similar CS value but different MDPG1$_{SSR}$10Kd genotype. Despite 'Y102' (*Aa*) and 'Kizuri' (*AA*) showed a similar CS value (1.186, 1.184), 'Kizuri' was characterized by a significant increase in 'juiciness' (6.9%) compared to 'Y102' (Welch Two Sample t-test, p value = 0.01). Similarly, the other cultivars showing an *Aa* genotype were less juicy compared with those characterized by similar CS values and *AA* genotype, with an increase in juiciness ranging from 5.4 % for 'Minneiska' (*AA*) compared to 'Red Delicious' (*Aa*) to 10.7 % for 'Fuji' (*Aa*) compared to 'Gala' (*AA*) (Figure 4). 'Juiciness' can be therefore associated to the combination of CS and the genotype at the *MdPG1 locus*. Similarly, 'juiciness' can result from the combination of either favourable MDPG1$_{SSR}$10KD genetic configuration and high CS values (angular cells) or from samples showing *Aa* genotype and low CS values (round cells). Even though 'Gala' and 'UEB32642' showed similar 'juiciness' (2.99 and 3 g respectively, Table 2), the first cultivar is characterized by Aa genotype and a CS value of 1.269, while 'UEB32642' showed a favourable *AA* genotype and a less favourable CS of 1.334. Similar patterns were also observed for 'Y102' and 'UEB6581' or for 'Red Delicious' and 'Gradisca'.

3.5 Sensory analysis

Fruit quality parameters related to texture, juiciness, flavour and aroma were also assessed using a sensory panel (Table 3). The standard deviations of the nine sensory descriptors showed a normal distribution (Shapiro-Wilk test: W = 0.91, p value = 0.37). 'MN55' was characterized by the highest sensory juiciness score

(79.5), in agreement with the correspondent instrumental measurement (Table 2). As for the sensory traits related to texture, 'Lumaga' showed the highest response in terms of crispness and crunchiness (67.2 and 71.5 respectively), while 'FEM16' and 'UEB6581' were characterized by the highest fibrousness and hardiness (73.5 and 74.7, respectively) (Table 3). As for the textural parameters that are generally negatively perceived by consumers, the apples showing the highest mealiness and granularity were 'Golden Delicious' and 'CIV323' (67.7 and 60.2 respectively). 'Gradisca' and 'Kizuri' were instead characterized by the highest flavour (62.4) and aroma (65.1) respectively (Table 3).

Results of both instrumental and sensory analysis were integrated in a PCA analysis (Figure 5A-B). The first two PCs explained the 76.6 % of the total phenotypic variability. The distribution of the cultivars along the two axes was in agreement with the results depicted in Figure 3, implying that the sensory measurements showed a high (direct or inverse) correlation with at least one of the traits measured instrumentally. The loadings related to 'Mealiness' and 'Granularity' pointed to the lower-left PCA quadrant, and both traits resulted inversely correlated with the mechanical components of texture (Figure 5; Supplementary Table 3). Sensory evaluated parameters, such as 'Flavour', 'Hardiness', 'Fibrousness', 'Crispness' and 'Crunchiness' were inversely correlated to 'Mealiness' and 'Granularity', as shown by the opposite loading projections and the correlation matrix, and positively correlated with the instrumentally measured mechanical parameters related to texture (Figure 5). 'Aroma' and 'Juiciness Sens.' showed orthogonal loadings projection compared with all the other sensory traits, implying a low correlation between these two sensory parameters and all the others (Figure 5). 'Sensory Juiciness' showed instead significant, positive, correlations, ranging from 0.6 ('Force Lin. Dis') to 0.8 ('Max Acoust. Pres.') with the instrumentally measured acoustic components of texture (Figures 5), with 'Kizuri' (PC1 = 2.91, PC2 -3.44), 'Gradisca' (PC1 = 2.29, PC2 = -1.07) and 'MN55' (PC1 = 4.59, PC2 = -1.42) showing the highest sensory juiciness values and optimal acoustic responses (Table 3, Supplementary Table 3). Both sensory and instrumental juiciness loadings pointed to the lower-right quadrant of the PCA (Figure 5A) with the two parameters showing a correlation of 0.54 (p value = 0.045) (Figure 5B). As for the cellular morphology parameters, CS resulted negatively correlated with the 'aroma' and 'juiciness' (cor = -0.37 and -0.31, respectively), while CA showed a direct correlation with both traits (cor

= 0.27 and 0.45, respectively). CA showed a different degree of association with the two type of juiciness assessed (instrumental and sensory), showing a weak indirect correlation and a direct correlation respectively. CS showed instead a more consistent behaviour, being inversely correlated to both measurements of juiciness. CA showed a high direct correlation with both the sensory traits related to texture, and the instrumentally measured mechanical components of texture. Overall, CS was inversely correlated with the instrumentally measured acoustic parameters, and a weak correlation with the mechanical parameters and the sensorially assessed texture (Figure 5 A-B).

Table 3: Sensory descriptors related to juiciness, texture, aroma and flavour for the fourteen accessions in analysis. Texture descriptors are either related to the physical (Hardiness, Mealiness, Granularity and Fibrousness) or acoustic response (Crispness, Crunchiness) of the fruit during mastication. The intensity of each descriptor was expressed as a score on a 100 mm linear scale, ranging from 0 (absence) to 100 (extremely intense).

Accession	Juiciness Sens.	Aroma	Crispness	Hardiness	Mealiness	Crunchiness	Granularity	Fibrousness	Flavour
Golden Delicious	32.3	45.2	20.9	11.5	67.7	12.9	60.1	8	45.9
Gala	34.2	47.8	29.6	25.4	56.3	17.6	53.4	12	40.3
CIV323	43.8	59.1	29.8	21	65.4	14.7	60.2	13.5	47.5
Red Delicious	45.7	60.1	44.8	23.9	61.5	24.7	48.8	26.3	37.9
Lumaga	48.3	55	65.5	71.8	8.4	53.4	14.1	68.9	45.4
Y102	52.3	50.9	57.3	68.1	10.6	53.6	26.3	57	49.1
UEB32642	53	53.7	58.4	51.1	29.2	48.8	35.6	37.8	56.1
Minneiska	54	56.8	25.8	17.8	56.2	14.6	57.9	11.7	39.7
FEM16	57.6	47.3	63.3	72.8	7.2	56.6	25.3	73.5	54.2
UEB6581	59.1	62	62.3	74.7	6	55.1	18	68	45.8
Fuji	62.5	50	53.8	46.9	18.6	38.3	34.8	47.6	43.2
Kizuri	63.2	65.1	50.9	43.7	19.2	43.1	32.3	39.4	47.2
Gradisca	66.3	45.8	55	58.5	7.1	52.1	22.5	54.1	62.4
MN55	79.5	65	67.2	72	5.6	71.5	16.2	72.7	49.8

3.6 Validation using X-ray computed micro-tomography

The tight correlation between cellular morphology and 'juiciness' was further confirmed by X-ray computed micro-tomography analysis. Example images are displayed in Figure 6 and Supplementary Figure 7. All cultivars showed a bimodal distribution of the log transformed volume of IS, with 'Golden Delicious', 'Fuji' and 'Kizuri' characterized by an increasing relative frequency of small over large IS, while 'Lumaga' showed a more uniform distribution of the IS spaces (Figure 7). This analysis supported and complemented the results obtained with the optical microscopy, confirming the interplay between CS and *MdPG1* allelism on the overall 'juiciness'. The seven cultivars depicted in Figure 7 were ordered according to their 'juiciness' in descending order and coloured according to their MDPG1$_{SSR}$10Kd genotype (*AA* = green, *Aa* = yellow). The elaboration of the 3D images analysis shows that

'juiciness' was influenced by the relative frequency of small IS within individuals showing the same MDPG1$_{SSR}$10Kd genetic background. Among the samples showing an *AA* genotype, cultivars like 'Kizuri' and 'Fuji' were characterized by both the highest fraction of small IS and the highest 'juiciness' values. In contrast, 'Lumaga' showed the lowest relative frequency of small IS and the lowest 'juiciness' while 'Minneiska' and 'Gradisca' were characterized by intermediate phenotypes for both traits. The same pattern was also observed within the two cultivars showing an *Aa* genotype with the higher juiciness of 'Golden Delicious' being accompanied by a higher fraction of small IS compared to 'Gala'. As observed in Figure 4, 'Fuji' and 'Golden Delicious' showed a similar cellular morphology but a substantial difference in 'juiciness' response (Figure 7, Table 2).

4 DISCUSSION

4.1 Analysis of the cellular morphology

Two complementary approaches were adopted to study cellular morphology focusing either on the cell (measuring CA and CS) or on the IS (measured by volume). While CA was slightly correlated with IS (cor = 0.24), the latter showed a higher positive correlation with CS (cor = 0.67).

412 The range of CA (33,137 μm^2 – 48,528 μm^2) was similar to what observed in previous work using the same
413 extraction protocol (McAtee et al., 2009), but was higher when compared to that using different cell
414 extraction and observation methods (Allan-Wojtas et al., 2003; Schotsmans et al., 2004) To this end it is in
415 fact interesting to underline that our study was based on observation made on whole cells, while most of the
416 works published to date were on the contrary based on light microscopy analysis carried out on fruit slices,
417 leading, therefore, to wrong cell size estimations, as already pointed out by McAtee et al. (2009).

418 The examination of the CS relied on the fact that previous analysis using confocal microscopy confirmed that
419 cell shape was not altered mechanically or osmotically during the cell isolation process (McAtee et al., 2009).
420 Interestingly, apples showing the highest fraction of round cells ('Kizuri', 'Y102') were also those
421 characterized by the lowest CS standard deviations and vice-versa (Figure 2B). The absence of cultivars
422 showing high CS (thus high fraction of elongated cells) and low standard deviation could be either due to the
423 sampling of elite germplasm or to the relative frequency of round cells that could not be lower than a certain
424 amount. Further studies on wider germplasm collections could better clarify this aspect.

425

426 **4.2 Comparison between instrumental and sensory data**

427 The fruit quality features were analysed across the accessions using instrumental and sensorial approaches.
428 Analytically measured juiciness was correlated with its sensory evaluation, validating the phenotyping
429 protocol employed in the study. Moreover, sensory juiciness showed the highest correlations with the
430 instrumentally measured acoustic parameters ('max acoustic pressure' and 'mean acoustic pressure'),
431 confirming the high relationship between acoustic response and juiciness (Daillant-Spinnler et al., 1996;
432 Allan-Wojtas et al., 2003; Corollaro et al., 2014a). However, the analytically measured juiciness showed the
433 highest correlation (-0.68) with CS, suggesting a specific role of cellular shape in influencing the apple
434 juiciness response. We believe that this is the first report of cellular shape influencing the juiciness of apple.
435 Even though the two measurements of juiciness were correlated, that between CS and sensory juiciness was
436 below the significance threshold. Further studies with larger germplasm collections and/or employing an

increased number of panellists, could help to elucidate the slightly different behaviour of the two measurements of juiciness. As for the correlation between cell size and the instrumentally measured texture parameters, CA was highly correlated with 'Yield force', which indicates the point of transition from the elastic (reversible) to the plastic phase (irreversible crushing) of the apple fruit flesh compression (Costa et al., 2011) (Figure 5B). Among the sensory parameters, CA, instead, showed the highest correlation (cor = 0.66, p value = 0.01) with 'Crispness', which represents the acoustic response of the fruit during the first bite. Combining both results, CA was more related to the instrumental and sensory parameters characterizing the first bite suggesting a role of CA in modulating the apple response when consumed fresh. Comparing the two parameters related to cell morphology, CA was directly related to the analytically measured textural parameters, while CS showed a differential pattern for the mechanical and acoustic parameters (being directly and inversely correlated to the two groups of traits, respectively) (Figure 5B). This aspect, coupled with the inverse correlation to 'Juiciness', made CS an ideal candidate to guide the selection of juicy and crispy apple fruit. Juiciness and cellular characteristics have also direct repercussion on apple flavour and aroma (Farneti et al., 2017). The direct correlation between aroma and 'juiciness' (and accordingly the inverse correlation between aroma and CS) can be reconducted to the fact that most of the volatiles that composes the apple aromatic *bouquet* are released (or *de novo* produced) upon cell breakage and consequent juice release. Thus, the selection of apple showing an increased fraction of round cells could result not only in higher juiciness but also in a better response in terms of aromatic production.

4.3 Effect of the *MdPG1* allelic variation on cell morphology

The depolymerization of the polysaccharide structure in the middle lamella is one of the major events affecting the texture response in apple (Atkinson et al., 2012; Ben-Arie and Kislev, 1979; Brummell, 2006). Our results confirmed the important role exerted by *MdPG1* and the direct correlation between the microsatellite marker designed in the proximity of this gene and textural features (supplementary Figure 5).

Even though MDPG1$_{SSR}$10Kd was not statistically associated with differences in juice release, cultivars showing an *AA* genotype were juicier than those with an *Aa* genotype (Supplementary Figure 6), suggesting a possible interplay between the physiological mechanisms governing the cell wall metabolism and the overall juiciness. Both analytical and sensory evaluation of fruit quality indicate that CS within each genotype categories affected overall apple juiciness (Figures 4, 7). Our hypothesis is that neither the cellular shape (or equally the size of the IS) nor MDPG1$_{SSR}$10Kd alone could explain the different response of accessions in terms of juiciness. The analysis of CS showed that similar values of 'juiciness' could be achieved, either with a high fraction of round cell and *Aa* or with a relatively lower fraction of round cell and *AA* (Figure 4). Thus, if not adequately considered as a cofactor, *MdPG1* could ultimately act as a confounding variable masking a real correlation between cell morphology and texture or juiciness. This is confirmed by the fact that the best performances in terms of juiciness were registered for accessions combining low CS value and *AA* genotype as shown for 'Kizuri' and 'MN55' (Table 2).

5 CONCLUSIONS

Economic success of an apple cultivar is determined by its juiciness and texture performances at harvest and after storage. Our results highlight that these factors are influenced by the combination of cellular morphology and the activity of *MdPG1* after storage. The role of cell shape (rather than cell size) influences juiciness, especially when the accessions are grouped according to their genotype at the MDPG1$_{SSR}$10Kd locus Nevertheless, further studies on wider germplasm is necessary to better elucidate the complex physiological regulation of juiciness and crispness. Taking the results presented here as a proof of concept, the establishment of an automated pipeline for an accurate phenotyping of the cell morphology could enable, in a close future, a valuable large screening tool for this feature.

Breeding programmes for juiciness often rely on the use of this marker for marker-assisted seedling selection (MASS) in light of the correlation between textural parameters and juiciness (King et al., 2000; Ulrich et al., 2014). Since the fruit texture is considered a fundamental trait in modern breeding programs, most of the

advanced selections are now homozygous for the favourable allele at this locus. Despite this favourable genetic configuration, breeding material showing a fixed *AA* genotype is still characterized by important differences in terms of texture and juiciness attributes, due to the polygenic regulation of such features. Furthermore, the use of this marker in breeding schemes for texture did not allow the selection of crispy over firm apple since *MdPG1* is linked to both components of texture. The identification of molecular markers linked to CS could greatly support the breeding for juiciness and aroma. The use of CS to guide the seedling selection could also allow a more precise analysis of the two textural components since CS showed a different pattern of correlation between the acoustic (prevalence of round cells) and mechanical (prevalence of elongated cells) texture parameters.

6. ACKNOWLEDGMENT

This work has been funded under the Program LP 6/99 art. 5 Autonomous Province of Trento by the CIF Project 'Apple & Berry'. The work was carried out in the frame of the PON "AIM: Attrazione e Mobilità Internazionale" No. 1808223-2 project.

7. REFERENCES

Abbott, J.A. 1999. Quality measurement of fruits and vegetables. Postharvest Biology and Technology 15: 207–225.

Allan-Wojtas, P.; Sanford, K.A.; Mcrae, K.B.; Carbyn, S. 2003. An integrated microstructural and sensory approach to describe apple texture. Journal of the American Society for Horticultural Science 128: 381–390.

Atkinson, R.G.; Sutherland, P.W.; Johnston, S.L.; Gunaseelan, K.; Hallett, I.C.; Mitra, D.; Brummell, D.A.; Schröder, R.; Johnston, J.W.; Schaffer, R.J. 2012. Down-regulation of POLYGALACTURONASE1 alters firmness , tensile strength and water loss in apple (*Malus x domestica*) fruit. BMC Plant Biology: 11–21.

Baumgartner, I.O.; Kellerhals, M.; Costa, F.; Dondini, L.; Pagliarani, G.; Gregori, R.; Tartarini, S.; Leumann, L.; Laurens, F.; Patocchi, A. 2016. Development of SNP-based assays for disease resistance and fruit quality traits in apple (*Malus × domestica* Borkh.) and validation in breeding pilot studies. Tree Genetics and Genomes 12: 12–35.

Ben-arie, R.; Kislev, N. 1979. Ultrastructural changes in the cell walls of ripening apple and pear fruit. Plant Physiology 64: 197–202.

Bertin, N.; Gautier, H.; Roche, C. 2001. Number of cells in tomato fruit depending on fruit position and source-sink balance during plant development. Plant Growth Regulation 57221: 1–8.

Bourne, M. 2002. Food texture and viscosity: concept and measurement. Elsevier.

Brummell, D.A. 2006. Cell wall disassembly in ripening fruit. Functional Plant Biology 33: 103–119.

Brummell, D.A.; Harpster, M.H. 2001. Cell wall metabolism in fruit softening and quality and its manipulation in transgenic plants. Plant Molecular Biology 47: 311–340.

Cappellin, L.; Farneti, B.; Di Guardo, M.; Busatto, N.; Khomenko, I.; Romano, A.; Velasco, R.; Costa, G.; Biasioli, F.; Costa, F. 2015. QTL analysis coupled with PTR-ToF-MS and candidate gene-based association mapping validate the role of Md-AAT1 as a major gene in the control of flavor in apple fruit. Plant

525 Molecular Biology Reporter 33: 239–252.

526 Charles, M.; Corollaro, M.L.; Manfrini, L.; Endrizzi, I.; Aprea, E.; Zanella, A.; Corelli Grappadelli, L.; Gasperi, F.
527 2018. Application of a sensory–instrumental tool to study apple texture characteristics shaped by
528 altitude and time of harvest. Journal of the Science of Food and Agriculture 98: 1095–1104.

529 Chen, P.M.; Borgic, D.M. 1985. Changes in water soluble polyuronides in the pulp tissue of ripening “Bosc”
530 pears following cold storage in air or in 1% oxygen. Journal of the American Society for Horticultural
531 Science 110.

532 Corollaro, M.L.; Aprea, E.; Endrizzi, I.; Betta, E.; Demattè, M.L.; Charles, M.; Bergamaschi, M.; Costa, F.;
533 Biasioli, F.; Corelli, L.; Gasperi, F. 2014a. A combined sensory-instrumental tool for apple quality
534 evaluation. Postharvest Biology and Technology 96: 135–144.

535 Corollaro, M.L.; Endrizzi, I.; Bertolini, A.; Aprea, E.; Demattè, M.L.; Costa, F.; Biasioli, F.; Gasperi, F. 2013.
536 Sensory profiling of apple: methodological aspects, cultivar characterisation and postharvest changes.
537 Postharvest Biology and Technology 77: 111–120.

538 Corollaro, M.L.; Gasperi, F.; Corelli Grappadelli, L. 2014b. An overview of sensory quality of apple fruit. Journal
539 of the American Pomological Society 68: 141–157.

540 Costa, F.; Cappellin, L.; Fontanari, M.; Longhi, S.; Guerra, W.; Magnago, P.; Gasperi, F.; Biasioli, F. 2012.
541 Texture dynamics during postharvest cold storage ripening in apple (*Malus* × *domestica* Borkh .).
542 Postharvest Biology and Technology 69: 54–63.

543 Costa, F.; Cappellin, L.; Longhi, S.; Guerra, W.; Magnago, P.; Porro, D.; Soukoulis, C.; Salvi, S.; Velasco, R.;
544 Biasioli, F.; Gasperi, F. 2011. Assessment of apple (*Malus* × *domestica* Borkh.) fruit texture by a
545 combined acoustic-mechanical profiling strategy. Postharvest Biology and Technology 61: 21–28.

546 Daillant-Spinnler, B.; MacFie, H.J.H.; Beyts, P.K.; Hedderley, D. 1996. Relationship beteen perceived sensory
547 properties and major preference directions of 12 varieties of apples from the southern hemisphere.
548 Food Quality and Preference 7: 113–126.

549 Endrizzi, I.; Torri, L.; Corollaro, M.L.; Demattè, M.L.; Aprea, E.; Charles, M.; Biasioli, F.; Gasperi, F. 2015. A
550 conjoint study on apple acceptability: sensory characteristics and nutritional information. Food Quality
551 and Preference 40: 39–48.

552 Farneti, B.; Di Guardo, M.; Khomenko, I.; Cappellin, L.; Biasioli, F.; Velasco, R.; Costa, F. 2017. Genome-wide
553 association study unravels the genetic control of the apple volatilome and its interplay with fruit
554 texture. Journal of Experimental Botany 68: 1467–1478.

555 Feldkamp, L.A.; Davis, L.C.; Kress, J.W. 1984. Practical cone-beam algorithm. Journal of the Optical Society of
556 America A 1: 612–619.

557 Fellows, I. 2012. A Data Analysis GUI for R. Journal of Statistical Software 49: 1–15.

558 Giovannoni, J. 2004. Genetic regulation of fruit development and ripening. The Plant Cell 16: 170–181.

559 Di Guardo, M.; Bink, M.C.A.M.; Guerra, W.; Letschka, T.; Lozano, L.; Busatto, N.; Poles, L.; Tadiello, A.; Bianco,
560 L.; Visser, R.G.F.; van de Weg, E.; Costa, F. 2017. Deciphering the genetic control of fruit texture in apple
561 by multiple family-based analysis and genome-wide association. Journal of Experimental Botany 68:
562 1451–1466.

563 Harker, F.R.; Gunson, F.A.; Jaeger, S.R. 2003. The case for fruit quality: an interpretive review of consumer
564 attitudes, and preferences for apples. Postharvest Biology and Technology 28: 333–347.

565 Harker, F.R.; Stec, G.H.; Hallett, I.C.; Bennett, C.L. 1997. Texture of parenchymatous plant tissue : a
566 comparison between tensile and other instrumental and sensory measurements of tksue strength and
567 juiciness. Postharvest biology and technology 5214: 63–72.

568 Kassambara, A.; Mundt, F. 2016. Factoextra: extract and visualize the results of multivariate data analyses. R
569 package version 1.

570 King, G.J.; Maliepaard, C.; Lynn, J.R.; Alston, F.H.; Durel, C.E.; Evans, K.M.; Griffon, B.; Laurens, F.; Manganaris,
571 A.G.; Schrevens, E.; Tartarini, S.; Verhaegh, J. 2000. Quantitative genetic analysis and comparison of
572 physical and sensory descriptors relating to fruit flesh firmness in apple (*Malus pumila* Mill.). Theoretical

and Applied Genetics 100: 1074–1084.

Lill, R.E.; Mespel, G.J. Van Der 1988. A method for measuring the juice content of mealy nectarines. Scientia Horticulturae 36: 267–271.

Longhi, S.; Moretto, M.; Viola, R.; Velasco, R.; Costa, F. 2012. Comprehensive QTL mapping survey dissects the complex fruit texture physiology in apple (*Malus x domestica* Borkh.). Journal of Experimental Botany 63: 1107–1121.

Longhi, S.; Cappellin, L.; Guerra, W.; Costa, F. 2013a. Validation of a functional molecular marker suitable for marker-assisted breeding for fruit texture in apple (*Malus × domestica* Borkh.). Molecular Breeding 32: 841–852.

Longhi, S.; Hamblin, M.T.; Trainotti, L.; Peace, C.P.; Velasco, R.; Costa, F. 2013b. A candidate gene based approach validates Md-PG1 as the main responsible for a QTL impacting fruit texture in apple (*Malus x domestica* Borkh). BMC plant biology 13: 37.

Mann, H.; Bedford, D.; Luby, J.; Tong, C. 2005. Relationship of instrumental and sensory texture measurements of fresh and stored apples to cell number and size. HortScience 40: 1815–1820.

McAtee, P.A.; Hallett, I.C.; Johnston, J.W.; Schaffer, R.J. 2009. A rapid method of fruit cell isolation for cell size and shape measurements. Plant Methods 5: 1–7.

Mendoza, F.; Verboven, P.; Mebatsion, H.K.; Kerckhofs, G. 2007. Three-dimensional pore space quantification of apple tissue using X-ray computed microtomography. Planta: 559–570.

Ng, J.K.T.; Schröder, R.; Sutherland, P.W.; Hallett, I.C.; Hall, M.I.; Prakash, R.; Smith, B.G.; Melton, L.D.; Johnston, J.W. 2013. Cell wall structures leading to cultivar differences in softening rates develop early during apple (*Malus x domestica*) fruit growth. BMC Plant Biology 13: 183.

Nybom, H.; Esselink, G.D.; Werlemark, G.; Vosman, B. 2003. Microsatellite DNA marker inheritance indicates preferential pairing between two highly homologous genomes in polyploid and hemisexual dog-roses, *Rosa* L. Sect. *Caninae* DC. Heredity 92: 139–150.

597 Olmstead, J.W.; Iezzoni, A.F.; Whiting, M.D. 2007. Genotypic differences in sweet cherry fruit size are
598 primarily a function of cell number. Journal of the American Society for Horticultural Science 132.

599 Quilot, B.; Genard, M. 2008. Is competition between mesocarp cells of peach fruits affected by the
600 percentage of wild species (*Prunus davidiana*) genome? Journal of Plant Research 121:55: 55–63.

601 Revelle, W.R. 2017. psych: Procedures for personality and psychological research title. [Online] Available:
602 https://cran.r-project.org/package=psych.

603 Ridler, T.; Calvard, S. 1978. Picture Thresholding Using an Iterative Selection Method. IEEE Transactions on
604 Systems, Man, and Cybernetics 8: 630–632.

605 Schindelin, J.; Arganda-Carreras, I.; Frise, E.; Kaynig, V.; Longair, M.; Pietzsch, T.; Preibisch, S.; Rueden, C.;
606 Saalfeld, S.; Schmid, B.; Tinevez, J.-Y.; White, D.J.; Hartenstein, V.; Eliceiri, K.; Tomancak, P.; Cardona, A.
607 2012. Fiji: an open-source platform for biological-image analysis. Nature Methods 9: 676–682. [Online]
608 Available: https://doi.org/10.1038/nmeth.2019.

609 Schotsmans, W.; Verlinden, B.E.; Lammertyn, J.; Nicolaï, B.M. 2004. The relationship between gas transport
610 properties and the histology of apple. Journal of the Science of Food and Agriculture 84: 1131–1140.

611 Seymour, G.B.; Manning, K.; Eriksson, E.M.; Popovich, A.H.; King, G.J. 2002. Genetic identification and
612 genomic organization of factors affecting fruit texture. Journal of experimental botany 53: 2065–2071.

613 Smedt, V. De; Pauwels, E.; Baerdemaeker, J. De; Nicolaı, B. 1998. Microscopic observation of mealiness in
614 apples : a quantative approach. Postharvest Biology and Technology 14: 151–158.

615 Ting, V.J.L.; Silcock, P.; Bremer, P.J.; Biasioli, F. 2013. X-ray micro-computer tomographic method to visualize
616 the microstructure of different apple cultivars. Journal of Food Science 78.

617 Ulrich, D.; Hoberg, H.; Fisher, C. 2014. Diversity and dynamic of sensory related traits in different apple
618 cultivars. Journal of Applied Botany and Food Quality 83: 70–75.

619 Wakasa, Y.; Kudo, H.; Ishikawa, R.; Akada, S.; Senda, M.; Niizeki, M.; Harada, T. 2006. Low expression of an
620 endopolygalacturonase gene in apple fruit with long-term storage potential. Postharvest Biology and

Technology 39: 193–198.

Waldron, K.W.; Parker, M.L.; Smith, A.C. 2003. Plant Cell Walls and Food Quality. Comprehensive reviews in food science and food safety 2.

Wickham, H. 2016. ggplot2: Elegant graphics for data analysis. Springer-Verlag New York. [Online] Available: https://ggplot2.tidyverse.org.

Figure 1: Boxplots of the 'juiciness' distribution within each of the fourteen samples.

Figure 2: Boxplot of the cell area (CA) (A) and cell size (CS) (B) distribution within the fourteen cultivars or advances selections.

Figure 3: PCA analysis of the instrumentally measured phenotypic data for 'juiciness', texture and cell morphology. (A) PCA scoring and loading plot; (B) heatmap of the pairwise correlations between the traits in analysis, correlations (B). values exceeding the significance threshold level (p value > 0.5) were crossed.

Figure 4: biplot representing the correlation between CS and 'juiciness'. Samples are coloured according to their genetic configuration at the $MDPG1_{SSR}$10KD locus as specified in legend; the overall linear regression linking the two variables is represented by a grey line while the linear regression made on the base of the two $MDPG1_{SSR}$10KD genotypes were represented in blue (*AA*) and pink (*Aa*) respectively.

Figure 5: PCA analysis of the instrumentally measured phenotypic data for 'juiciness', texture and cell morphology and the sensory data. (A) PCA scoring and loading plot. (B) Pairwise correlations plot , traits that were evaluated instrumentally or through a sensory panel are labelled in green and violet respectively. Values exceeding the significance threshold level (p value > 0.5) were crossed.

Figure 6: Cross-sectional slice obtained after tomographic reconstruction (A). Binary image displaying the segmented intercellular spaces in white (B). 3D rendering of a reconstructed cylindrical sample (C).

Figure 7: Histograms of the log transformed volume of the intercellular space. Samples are coloured according to their genetic configuration at the MDPG1 SSR10Kd *locus* (yellow = *Aa*, green = *AA*). For each

accession, the density distribution of the three fruits analysed for each cultivar is depicted as blue, green and red continuous lines.

Supplementary Figure 1: Texture profiling of the 14 apple cultivars stored under normal atmospheric conditions. The distribution of each texture parameter (both as histogram and as density fitted line) is represented on the diagonal. On the lower triangle the bivariate scatter plots and the relative fitted line (red continuous line) are depicted while the respective absolute correlation values are reported on the upper triangle.

Supplementary Figure 2: Principal component analysis of the textural parameters; A: Scoreplot of the first two principal components, individuals are coloured according to their qualities of representation, B: loading plots of the ten variables used to compute the principal component analysis, arrows are coloured according to the type of variables (acoustic or mechanic). (C) barplot representing the percentage of the explained variance of all computed dimensions (principal components). The boxplot of the two variables showing the most divergent loading scores and grouped by cultivars are represented in D ('Final force') and E ('Number of force peaks').

Supplementary Figure 3: Analysis of the cellular morphology on the germplasm in analysis. The distribution of each of the four parameters (both as histogram and as density fitted line) is represented on the diagonal. On the lower triangle the bivariate scatter plots and the relative fitted line (red continuous line) are depicted while the respective absolute correlation values are reported on the upper triangle.

Supplementary Figure 4: For each cultivar, the average cell area (CA, y axis) is calculated for ten subsets of increasing size ranging from 10 cells to the total number of cells analysed (x axis). For each sample sizes, 100 random samplings were extracted, the respective average area calculated, and its distribution plotted (grey boxplots). The red, horizontal line represents, for each cultivar, the average value of the cell area when all cells are considered, cultivars are ordered from left to right and from top to bottom according to the quantity of extracted juice.

669 Supplementary Figure 5: Boxplots of the 10 textural parameters analysed. Traits that are related to
670 mechanical or acoustic parameters are coloured in blue or red respectively. For each trait, individuals are
671 grouped according to their genotype at the MDPG1 SSR10Kd *locus* (heterozygous =:*Aa*, homozygous = *AA*).

672 Supplementary Figure 6: Boxplots of the 'juiciness' explained by the genotype at the MDPG1 SSR10Kd *locus*
673 (heterozygous = *Aa*, homozygous = *AA*).

674 Supplementary Figure 7: Virtual slicing of a sample of the 'Kizuri' cultivar, reconstructed by X-ray
675 microtomography.

676

Figure 1

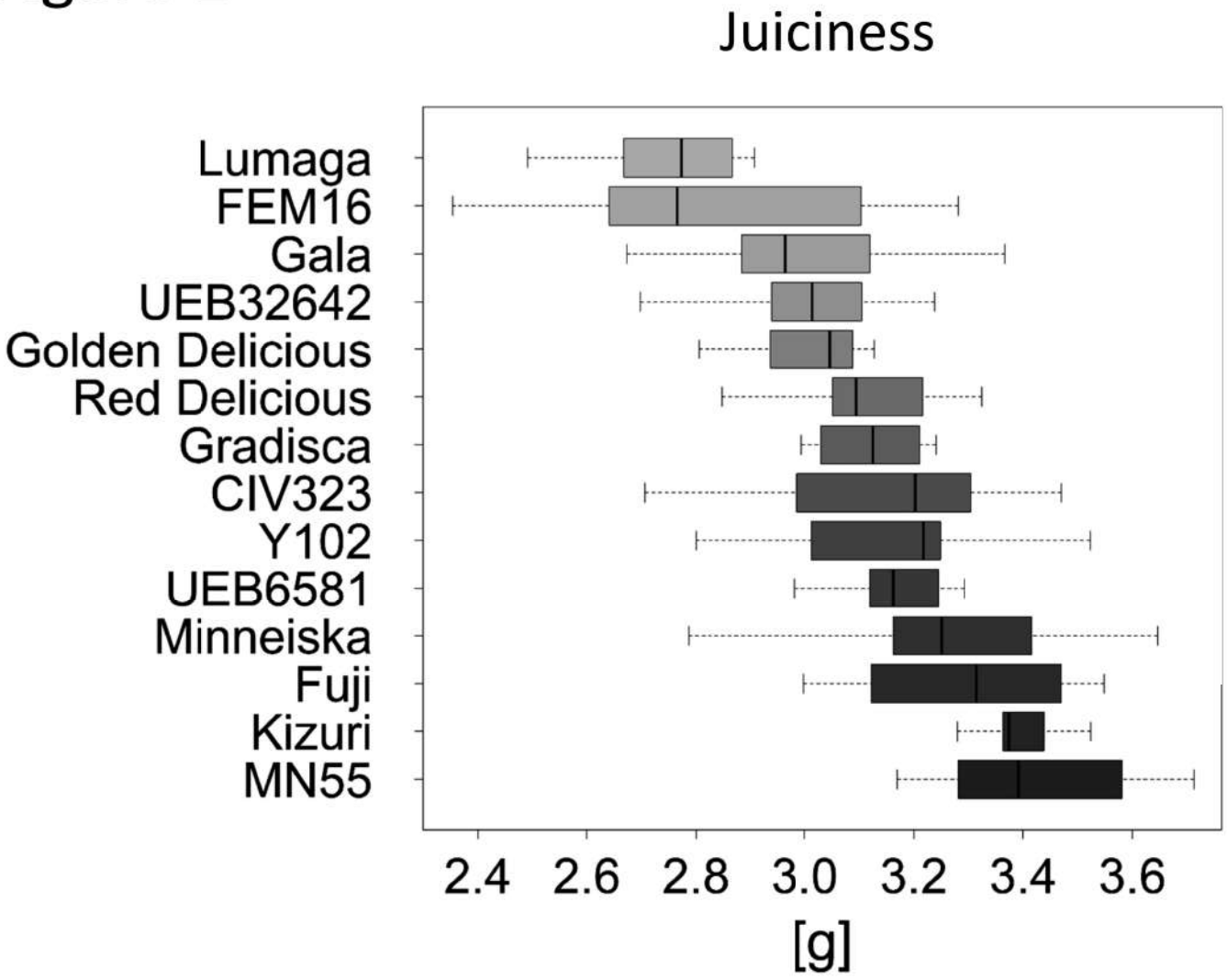
Juiciness
Lumaga
FEM16
Gala
UEB32642
Golden Delicious
Red Delicious
Gradisca
CIV323
Y102
UEB6581
Minneiska
Fuji
Kizuri
MN55
2.4
2.6
2.8
3.0
3.2
3.4
3.6
[g]

Figure 2

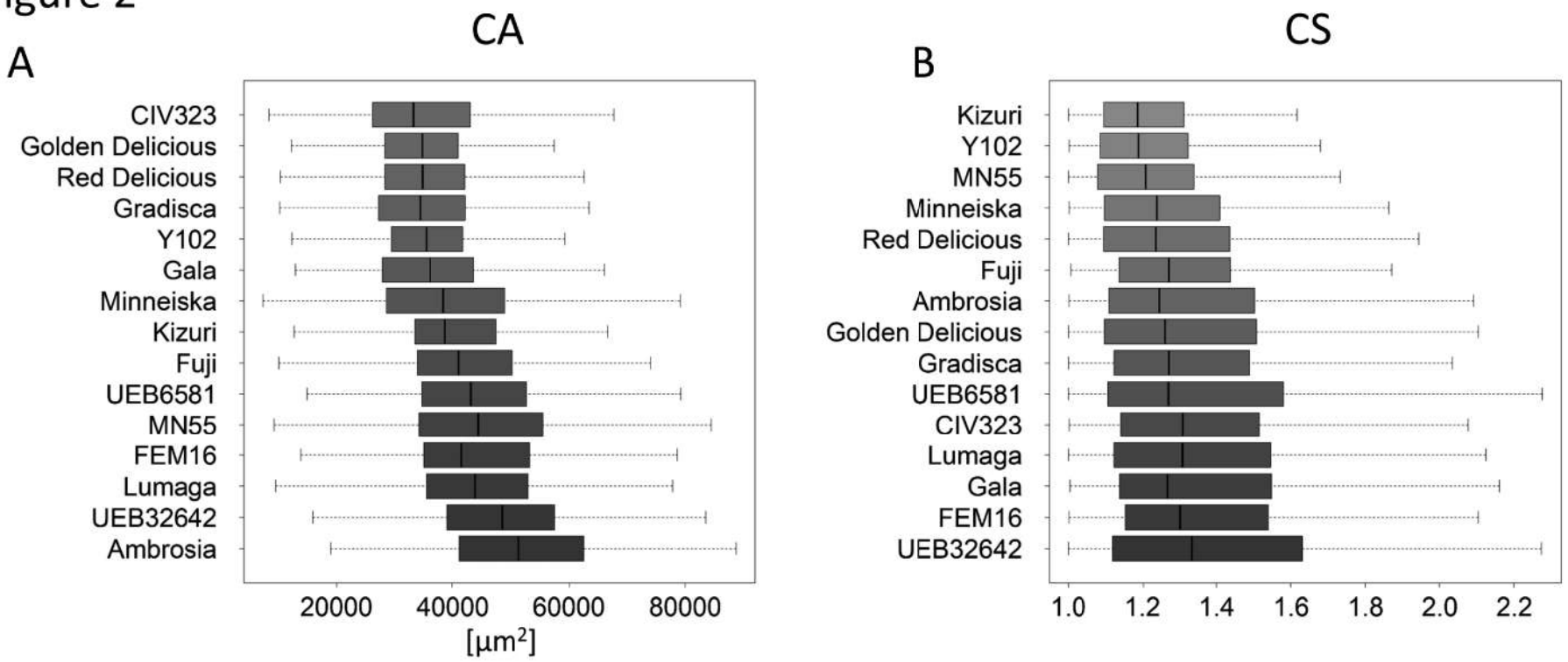
A
CA
CIV323
Golden Delicious
Red Delicious
Gradisca
Y102
Gala
Minneiska
Kizuri
Fuji
UEB6581
MN55
FEM16
Lumaga
UEB32642
Ambrosia
20000
40000
60000
80000
[µm²]
B
CS
Kizuri
Y102
MN55
Minneiska
Red Delicious
Fuji
Ambrosia
Golden Delicious
Gradisca
UEB6581
CIV323
Lumaga
Gala
FEM16
UEB32642
1.0
1.2
1.4
1.6
1.8
2.0
2.2

Figure 3

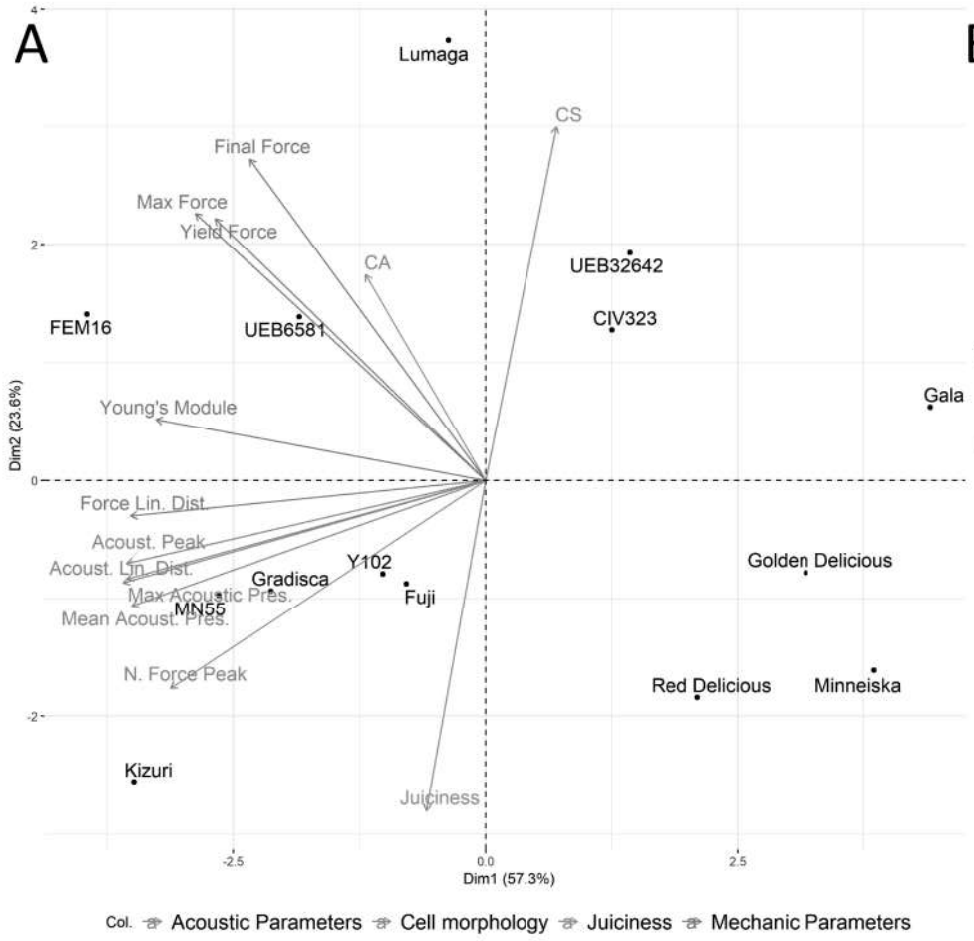
A
Lumaga
CS
Final Force
Max Force
Yield Force
CA
UEB32642
FEM16
UEB6581
CIV323
Gala
Young's Module
Force Lin. Dist.
Acoust. Peak
Acoust. Lin. Dist.
Gradisca
Y102
Golden Delicious
Max Acoustic Pres.
MN55
Fuji
Mean Acoust. Pres.
N. Force Peak
Red Delicious
Minneiska
Kizuri
Juiciness
Dim2 (23.6%)
Dim1 (57.3%)
Col. Acoustic Parameters Cell morphology Juiciness Mechanic Parameters

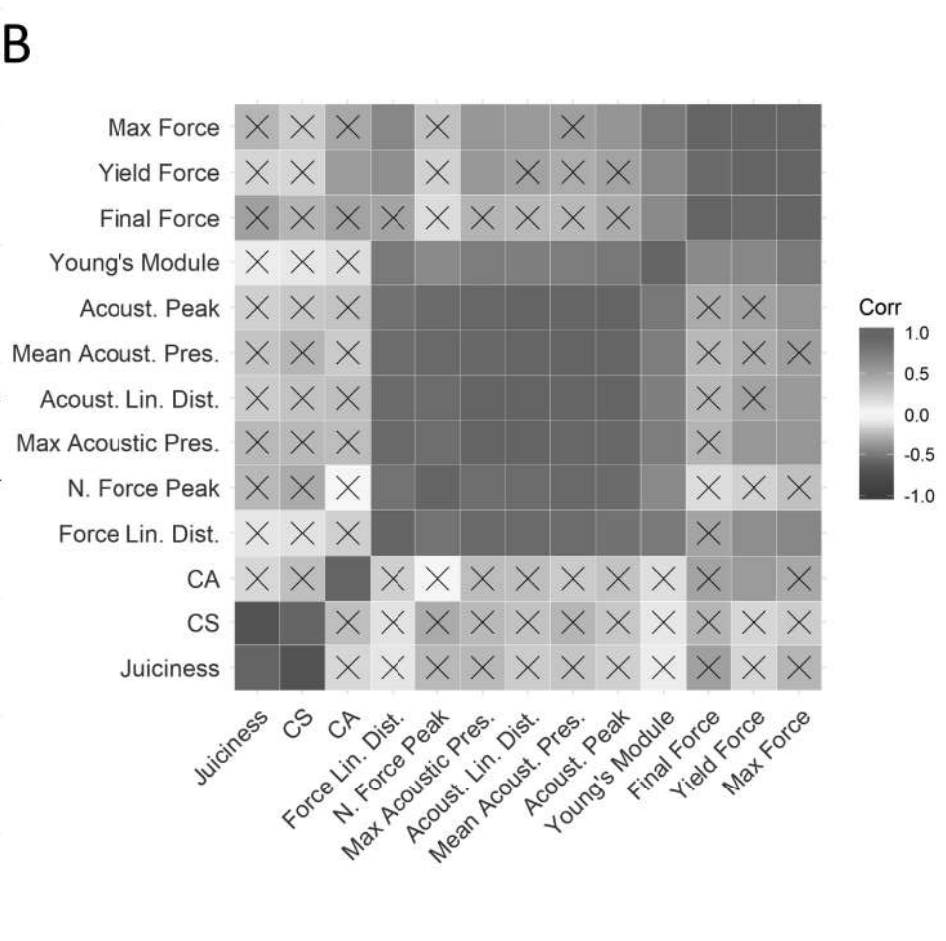
B
Max Force
Yield Force
Final Force
Young's Module
Acoust. Peak
Mean Acoust. Pres.
Acoust. Lin. Dist.
Max Acoustic Pres.
N. Force Peak
Force Lin. Dist.
CA
CS
Juiciness
Corr
1.0
0.5
0.0
-0.5
-1.0

Figure 4

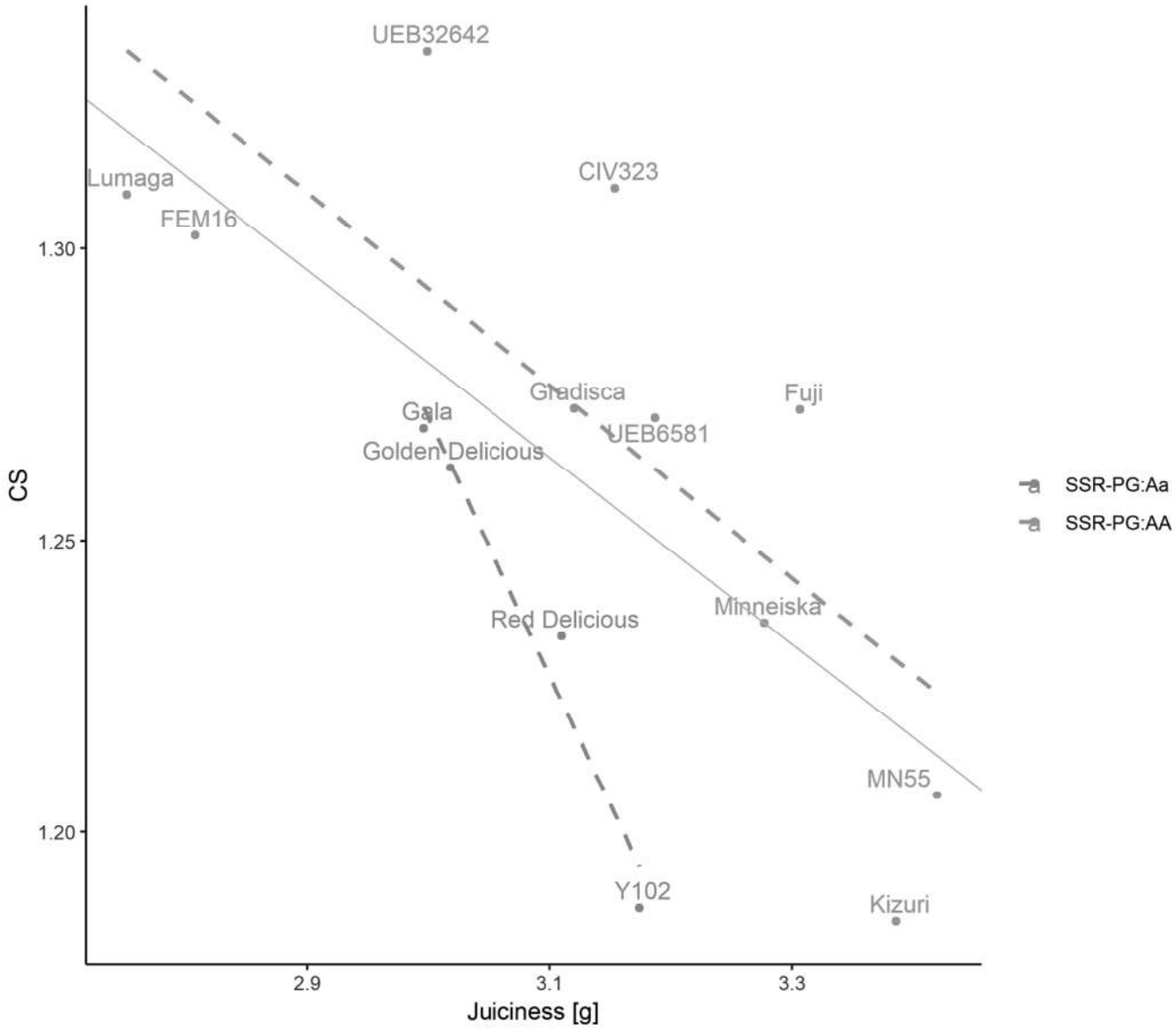
UEB32642
CIV323
Lumaga
FEM16
1.30
Gradisca
Fuji
Gala
UEB6581
Golden Delicious
CS
1.25
Minneiska
Red Delicious
MN55
1.20
Y102
Kizuri
2.9
3.1
3.3
Juiciness [g]
SSR-PG:Aa
SSR-PG:AA

Figure 5

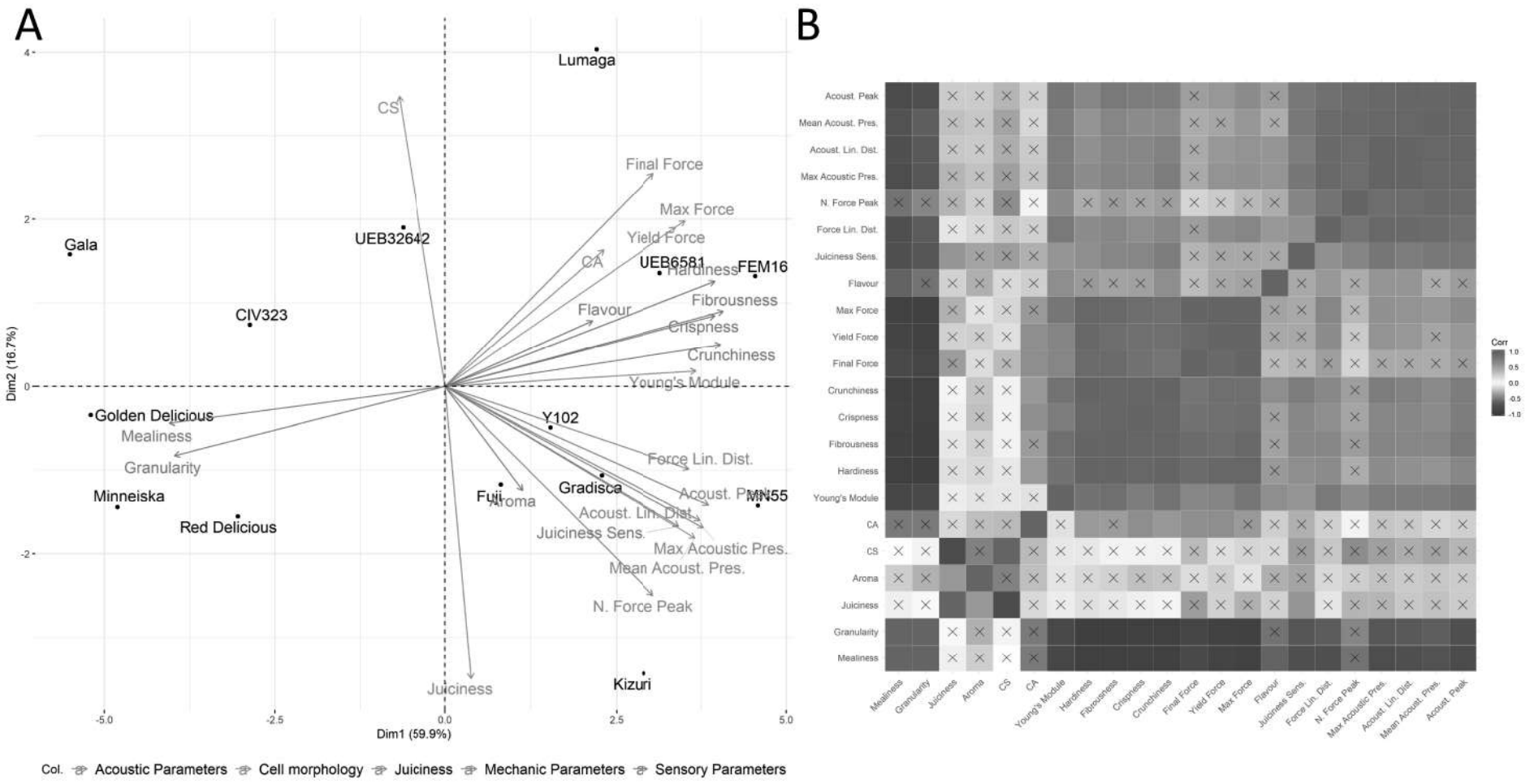
A
B
Lumaga
CS
Final Force
Max Force
Yield Force
Gala
UEB32642
CA
UEB6581
Hardiness
FEM16
Fibrousness
Flavour
CIV323
Crispness
Crunchiness
Young's Module
Golden Delicious
Mealiness
Granularity
Y102
Force Lin. Dist.
Minneiska
Fuji
Aroma
Gradisca
Acoust. Peak
MN55
Acoust. Lin. Dist.
Red Delicious
Juiciness Sens.
Max Acoustic Pres.
Mean Acoust. Pres.
N. Force Peak
Juiciness
Kizuri
Dim2 (16.7%)
Dim1 (59.9%)
Col. Acoustic Parameters Cell morphology Juiciness Mechanic Parameters Sensory Parameters
Corr

Figure 6

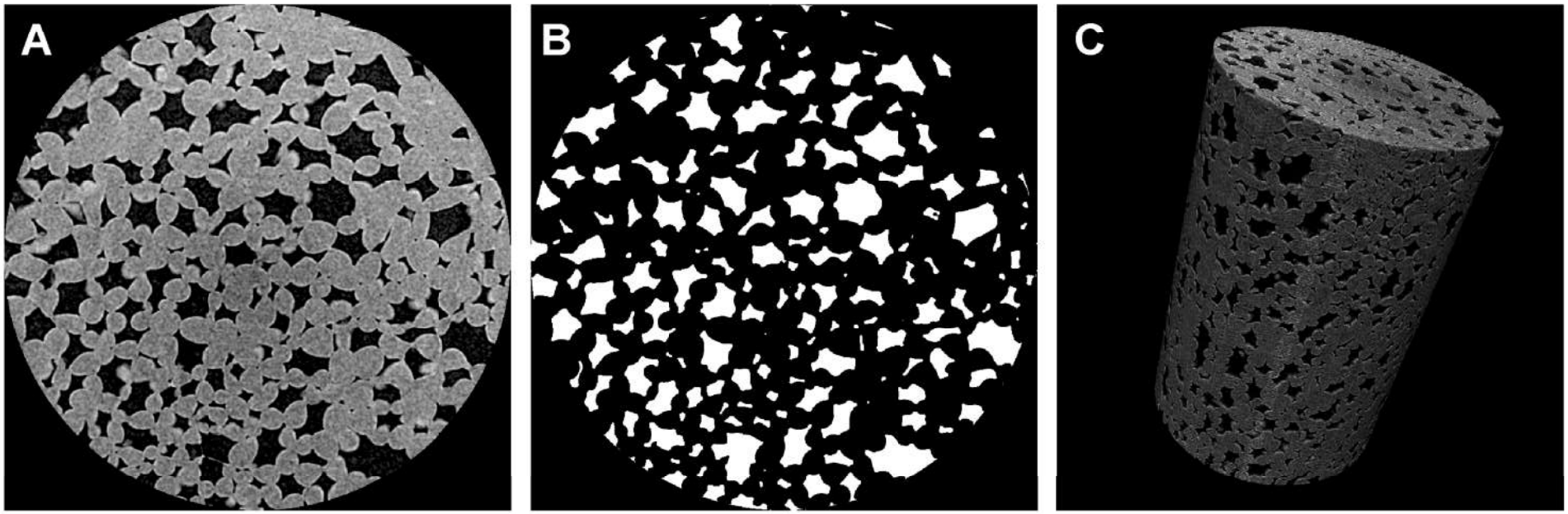

Figure 7

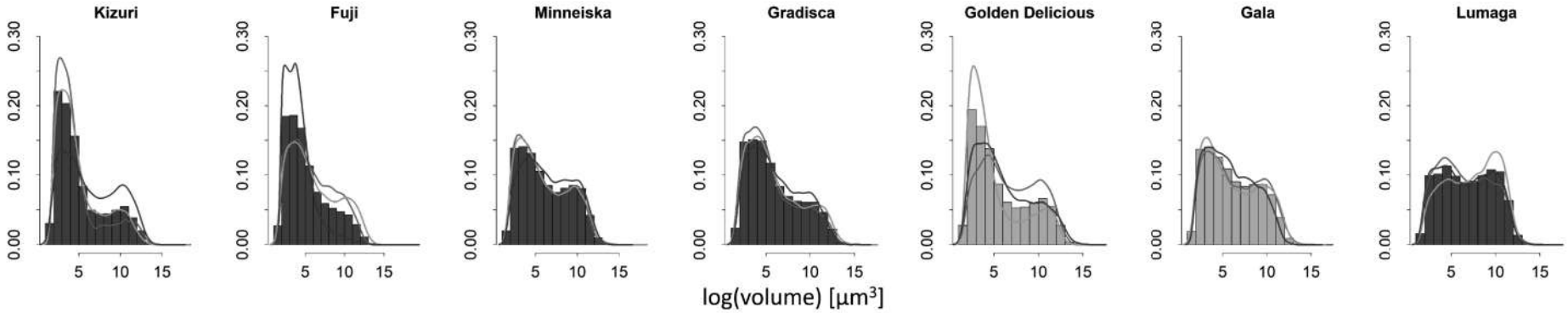
Kizuri
Fuji
Minneiska
Gradisca
Golden Delicious
Gala
Lumaga
0.00
0.10
0.20
0.30
5
10
15
log(volume) [µm³]

Supplementary Figure 1

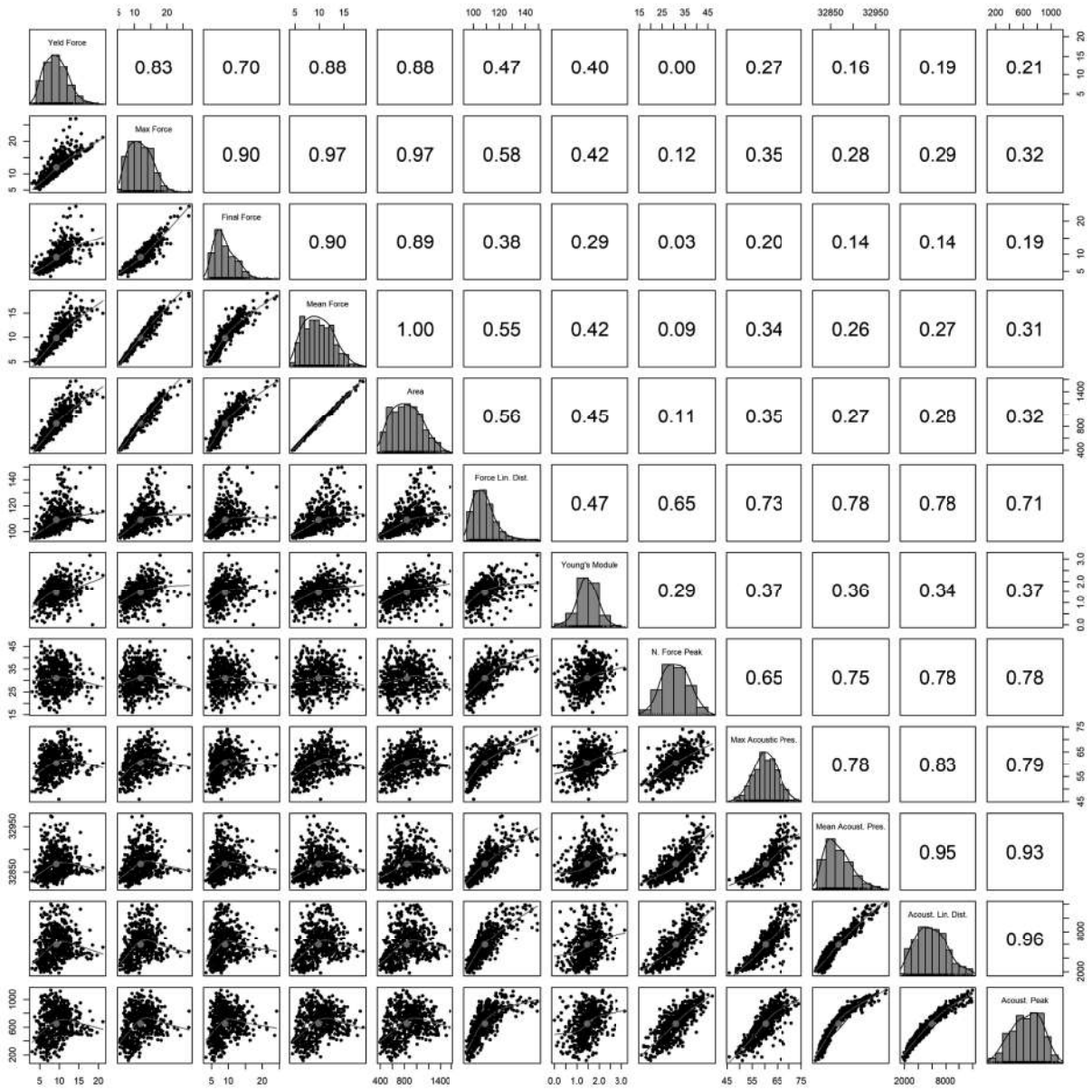

Supplementary Figure 2

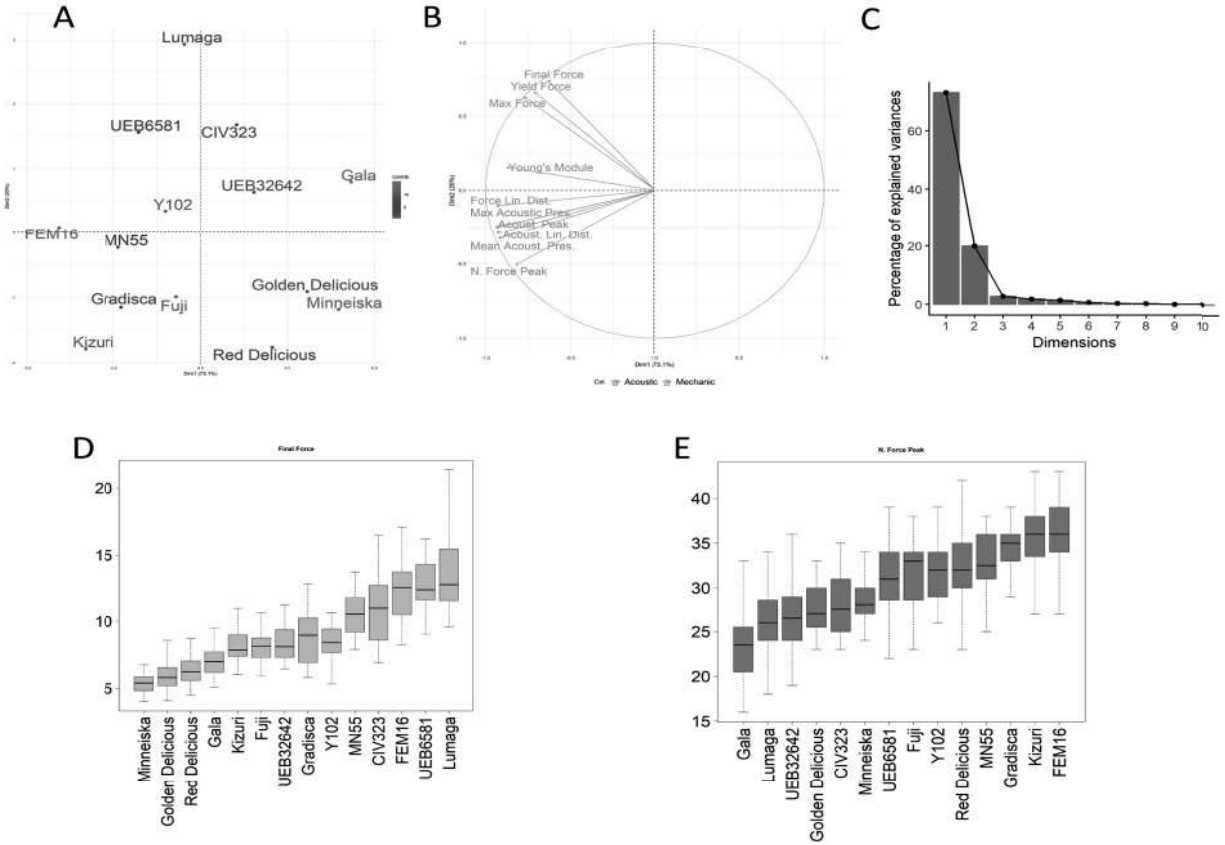

Supplementary Figure 3

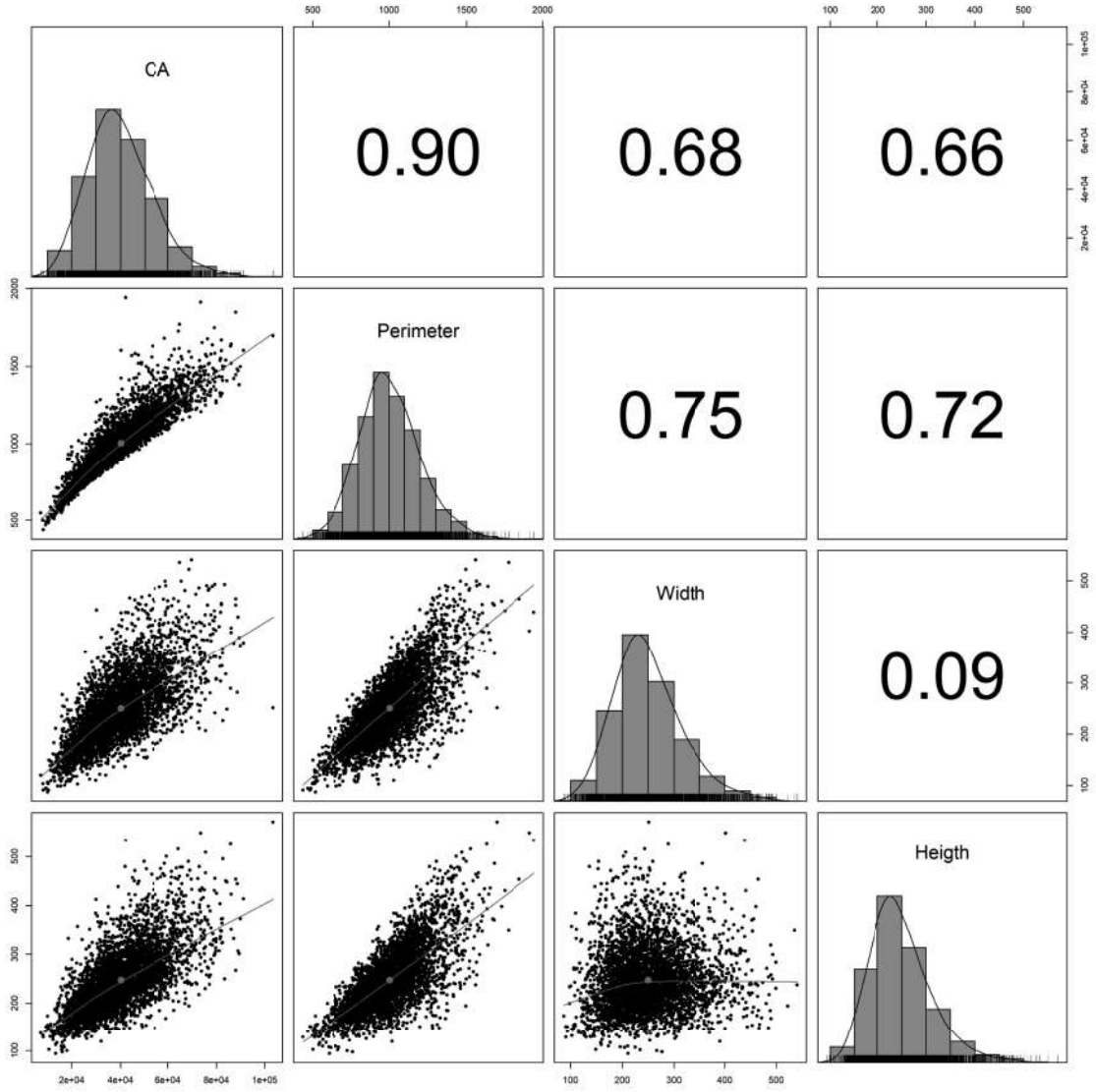

Supplementary Figure 4

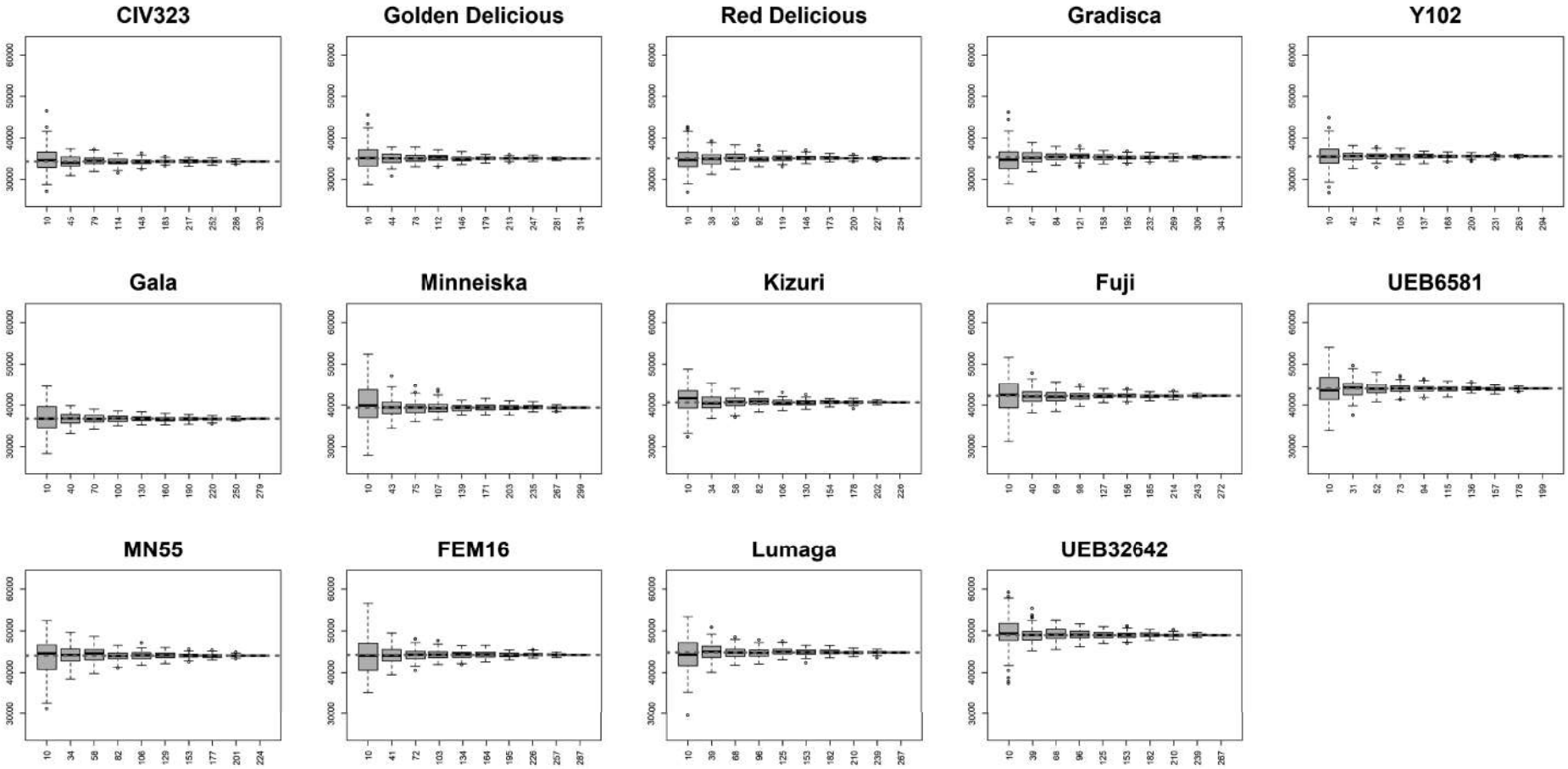

Supplementary Figure 5

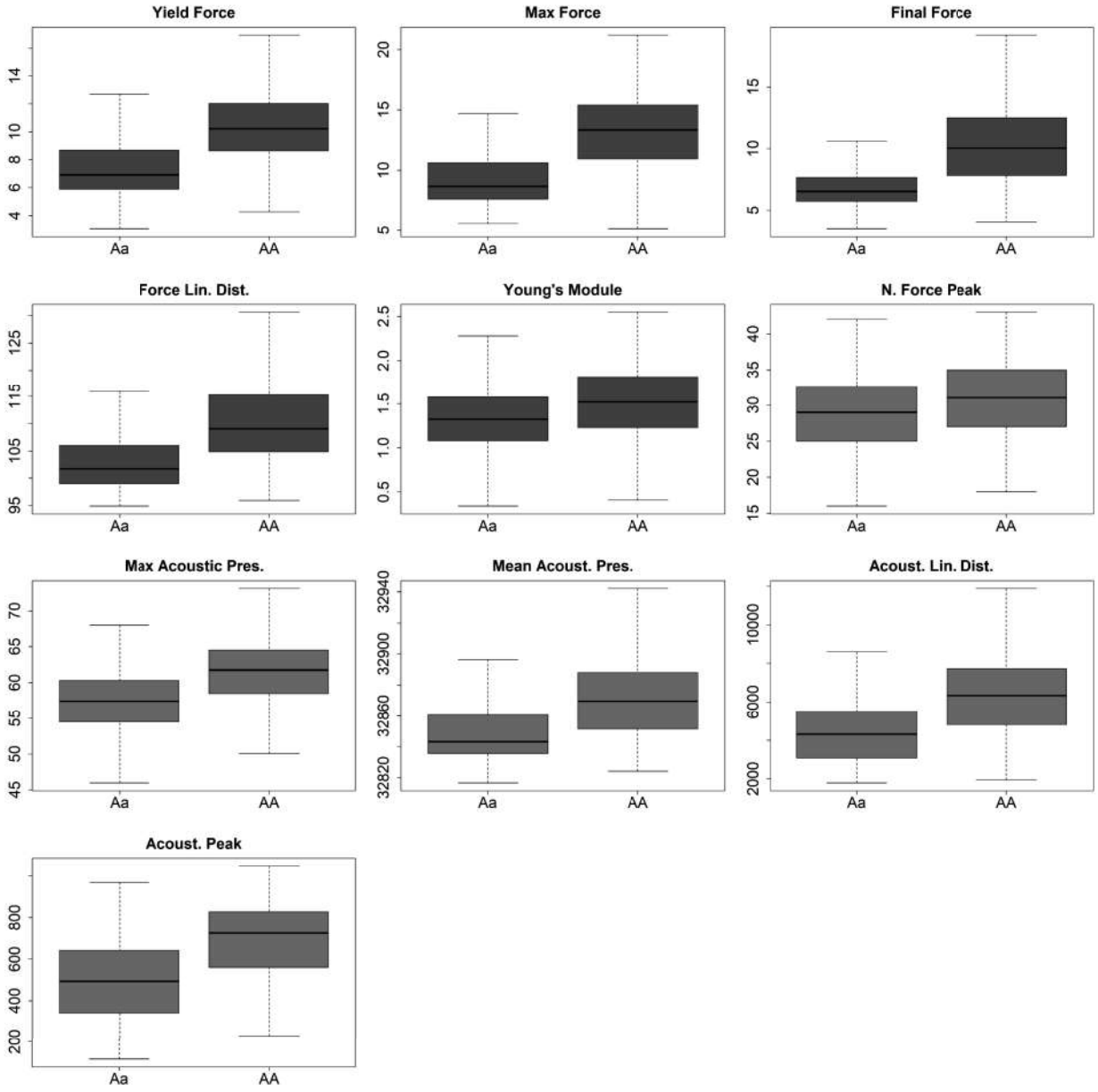

Supplementary Figure 6

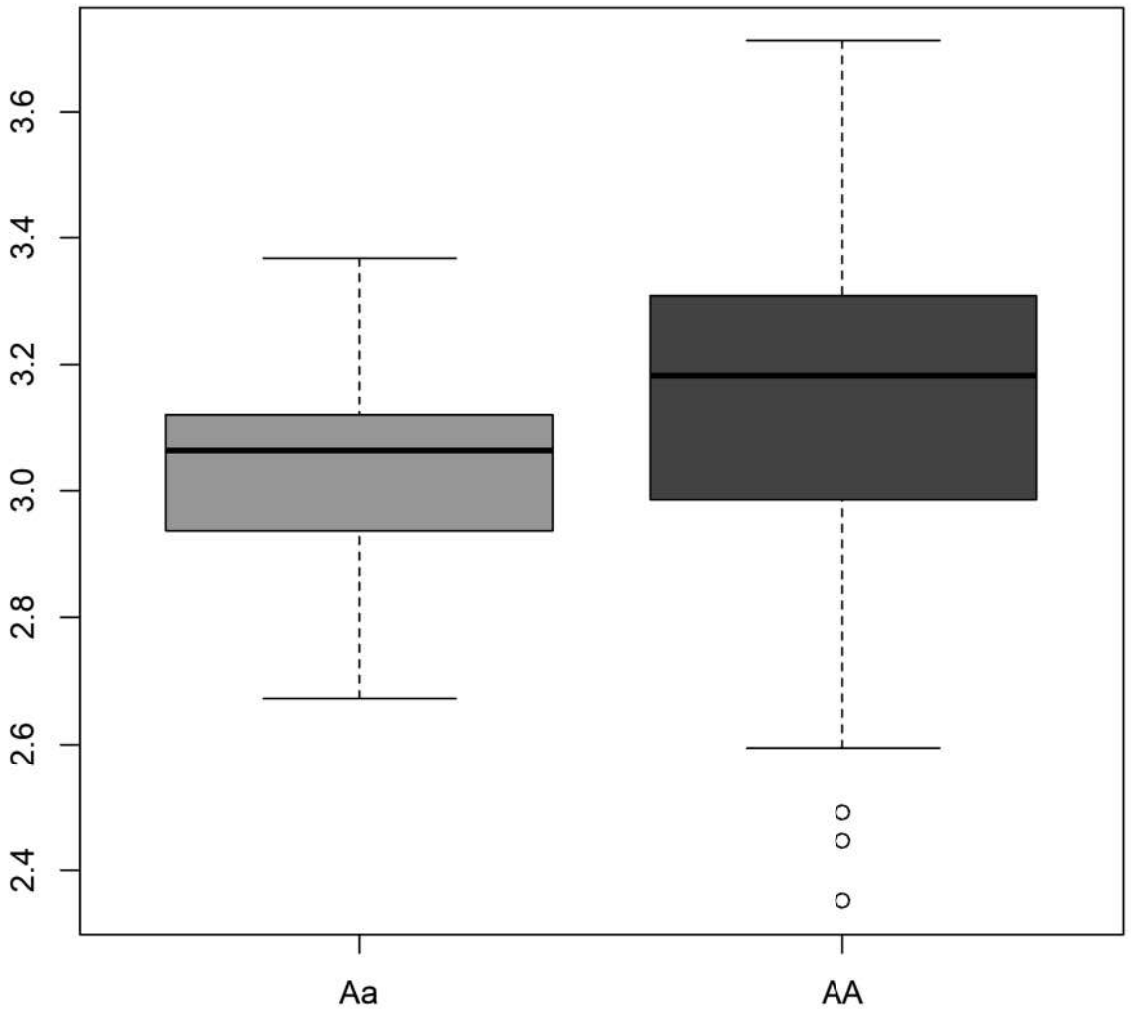

Supplementary Table 1: Description of the size of the disks (or cubes for light microscopy) used for the phenotypic analysis. Fer each analysis the number of fruits and disk/fruit is reported.

	Diameter-Side [cm]	Volume [cm^3]	Fruits	Disk/fruit
Juiciness	1	0.785	3	3
Texture	1	0.785	≥5	3
Light microscopy	1	1	3	1
Micro tomography	0.6	0.226	3	1
Sensory	1.8	2.544	16	1

Supplementary Table 2: The sensory lexicon developed by the panel for descriptive analysis of apples: For each descriptor, the sensory definition is shown.

Descriptors	Sensory definition
Aroma	Overall odour sensation orto-nasally perceived (by smelling the sample)
Crispness	Sound (pitch/intensity) produced by the sample at the first bite using the incisors
Hardness	Resistance of the sample to the first chews with molars (1-2 chews without breaking it)
Juiciness	Amount of juice released during chewing the sample (first 3 chews)
Mealiness	Degree of flesh breaking in small and dry fragments/granules during chewing
Crunchiness	Sound (pitch/intensity) produced by the sample during 5 molar chews
Granularity	Numbers/size of fragments/granules produced during chewing
Fibrousness	Degree of flesh breaking during chewing in thick and fibrous fragments/granules
Flavour	Overall flavour (odour) sensation retro-nasally perceived (by tasting the sample)

Supplementary table 3: Individuals' scores of the principal component analysis performed: PCA – Texture refers to supplementary Figure 2; PCA - Texture, Juiciness, Cell Morphology refers to Figure 3A, PCA - Texture, Juiciness, Cell Morphology, Sensory analysis refers to Figure 5A

Samples	PCA - Texture		PCA - Texture, Juiciness, Cell Morphology		PCA - Texture, Juiciness, Cell Morphology, Sensory analysis	
	PC1	PC2	PC1	PC2	PC1	PC2
CIV323	1.04	1.68	1.27	1.2	-2.87	0.74
FEM16	-4.09	0.09	-3.97	1.62	4.54	1.32
Fuji	-0.70	-0.99	-0.83	-1.05	0.82	-1.17
Gala	4.33	0.8	4.48	0.95	-5.5	1.58
Golden Delicious	3.07	-0.91	3.19	-0.84	-5.2	-0.34
Gradisca	-2.28	-1.15	-2.09	-0.87	2.29	-1.07
Kizuri	-3.32	-1.79	-3.53	-2.55	2.91	-3.44
Lumaga	-0.46	2.94	-0.4	3.65	2.21	4.03
Minneiska	3.97	-1.19	3.83	-1.67	-4.81	-1.44
MN55	-2.37	-0.23	-2.65	-1.16	4.59	-1.42
Red Delicious	2.06	-1.77	2.13	-1.76	-3.04	-1.56
UEB32642	1.54	0.64	1.37	1.66	-0.62	1.9
UEB6581	-1.77	1.56	-1.81	1.61	3.15	1.36
Y102	-1	0.34	-0.99	-0.79	1.54	-0.49

Declaration of interests

 The authors declare that they have no known competing financial interests or personal relationships that could have appeared to influence the work reported in this paper.

☐The authors declare the following financial interests/personal relationships which may be considered as potential competing interests:

Poles L: Conceptualization, Methodology, Investigation, Writing - Original Draft; **Gentile A**: Investigation, Writing - Review & Editing; **Giuffrida A**: Investigation; **Valentini L**: Investigation; **Endrizzi I**: Investigation; **Aprea E**: Investigation, **Gasperi F**: Investigation, Writing - Review & Editing, Resources; **Distefano G**: Investigation, Writing - Review & Editing; **Artioli G**: Writing - Review & Editing; **La Malfa S**: Writing - Review & Editing, Resources; **Costa F**: Writing - Review & Editing**; Lovatti F**: Conceptualization, Resources, Writing - Review & Editing, Funding acquisition; **Di Guardo M**: Conceptualization, Formal analysis, Writing - Original Draft, Writing - Review & Editing, Supervision